J. Physiol. (1986), **373**, *pp.* 129–162
With 12 *text-figures*
Printed in Great Britain

ACTIVATION OF ACETYLCHOLINE RECEPTORS ON CLONAL MAMMALIAN BC3H-1 CELLS BY LOW CONCENTRATIONS OF AGONIST

BY STEVEN M. SINE* AND JOE HENRY STEINBACH†

From the Salk Institute, P.O. Box 85800, San Diego, CA 92138 and the † Department of Anesthesiology, Washington University School of Medicine, 660 South Euclid Avenue, St. Louis, MO, 63110, U.S.A.

(*Received 15 May 1985*)

SUMMARY

1. The patch-clamp technique was used to examine the activation of single acetylcholine receptor channels of clonal BC3H-1 mouse muscle cells. Single-channel currents were activated by low concentrations of the strong agonists acetylcholine (ACh, 50–100 nM), carbamylcholine (1–2 μM), and suberyldicholine (30–50 nM).

2. At low agonist concentrations channel openings occur as isolated short-duration openings and as bursts of longer duration openings separated by brief closed periods.

3. Two distinct types of brief closed periods separate long duration openings: brief closures (mean duration, 50 μs) and intermediate closures (mean duration, 0·5–1·0 ms).

4. The kinetic properties of intermediate closures depend on the agonist, suggesting that they reflect receptor reopening from the closed state leading to the open state. Properties of brief closures, in contrast, are independent of the agonist, indicating that they result from an additional closed state leading away from the pathway producing the open state.

5. A receptor activation scheme is proposed which accounts for the observed closed states, and transition rate estimates are presented for steps within the proposed scheme.

6. The channel opening rate, β, differs several-fold for the agonists studied (200–1400 s^{-1}) and is comparable to the dissociation rate, k_{-2} (900 s^{-1}). The dissociation rate is similar for the three agonists studied. The channel closing rate, α, is much slower than the opening rate (20–60 s^{-1}). The probability is high that a doubly liganded channel is in the open state and depends on the agonist (0·75–0·97).

7. β increases and α decreases at more negative membrane potentials, whereas k_{-2} shows little potential dependence.

INTRODUCTION

At the vertebrate motor synapse the acetylcholine receptor (AChR) links the binding of acetylcholine molecules to activation of its ion channel. Magleby & Stevens

* Present address: Department of Physiology and Biophysics, Yale University School of Medicine, New Haven, CT, 06510, U.S.A.

(1972) suggested a scheme in which the binding of agonist is rapid and at equilibrium, whereas changes in channel conformation are slower, with an opening rate, β, and closing rate, α. In the past decade, experiments have supported expanded versions of this two-step scheme, and transition rate estimates have been obtained for reaction steps within these schemes (Steinbach, 1980; Adams, 1981). However, the precise mechanism of receptor activation remains elusive, and it is still debated whether receptor activation is limited by agonist binding steps or by channel conformational changes.

With the single-channel recording technique it is now possible to observe directly the occurrence of open and closed receptor states and to estimate the rates of transition between these states. Colquhoun & Hawkes (1981) proposed that at low agonist concentrations currents through receptor channels would appear as bursts of several openings separated by brief closed periods. Such burst-like behaviour is predicted by a scheme in which the channel opening rate, β, is comparable to the rate of dissociation of agonist, k_{-2}, enabling channels to close and reopen several times before the agonist dissociates. Estimates of β and k_{-2}, then, may be obtained through the analysis of brief closures within bursts. Brief closures have been analysed quantitatively but different estimates of β and k_{-2} have been reported (Colquhoun & Sakmann, 1981; Dionne & Leibowitz, 1982; Sine & Steinbach, 1984*a*). In these studies it has been generally assumed that the closed dwell times under analysis correspond to the closed states underlying receptor activation processes. Given such a disparity in the estimated rate constants, it becomes particularly important to demonstrate that the closed dwell times are clearly associated with receptor activation processes.

There are several ways of identifying the closed dwell times involved in receptor activation processes. First, activation appears to be agonist-specific, as suggested by the wide range of dissociation constants for agonist binding and from differences in apparent mean open times (Katz & Miledi, 1973; Sine & Taylor, 1979). Thus, activation processes should be reflected by the appearance of brief closures which exhibit agonist specificity. Secondly, measurements at low agonist concentrations make quantitative predictions for activation kinetics at intermediate and high agonist concentrations (Colquhoun & Hawkes, 1981). Therefore, the closed times reflecting receptor activation processes may be identified on the basis of their agonist specificity and dependence on agonist concentration.

In the present study the patch-clamp technique was used to examine the activation of AChR channels on BC3H–1 clonal muscle cells. BC3H–1 cells are well suited for these experiments because ligand binding and tracer ion flux measurements have defined the low and high agonist concentration ranges for activation of these receptors (Sine & Taylor, 1979, 1980, 1981). In this paper, receptor activation is examined in the presence of low concentrations of ACh, carbamylcholine and suberyldicholine. For each agonist, a short-duration closed state is identified, which appears to result from receptor activation processes. Analysis of these brief closures provides estimates for the transition rate constants, β and k_{-2}. A subsequent paper describes the analysis of measurements obtained at high agonist concentrations (S. M. Sine & J. H. Steinbach, in preparation).

METHODS

BC3H–1 cells were prepared for experiments as described previously (Sine & Steinbach, 1984*a*, 1986). Cells for experiments were grown on glass cover-slips in Dulbeccos Modified Eagles Medium (DME) supplemented with 0·5% cadet calf serum (0·5% DME) and treated with proteolytic enzymes on day 5 or 6 in culture. The enzyme treatment was accomplished in two steps. First, the cells were rinsed free of serum (2 × 5 ml washes with DME) and covered with collagenase (150 u./ml in HEPES-buffered DME, CS III Worthington) for 30 min at 21 °C. The cells were immediately rinsed (1 × 5 ml wash with DME) and covered with pancreatin solution (2% in DME, Grand Island Biochemicals, Chagrin Falls, OH) until the cells became rounded (usually 3–5 min). The cells were rinsed free of enzyme (1 × 5 ml wash with 0·5% DME), covered with 0·5% DME, and returned to the incubator for 6–7 days. The medium was replaced with fresh 0·5% DME 1 or 2 days before recording agonist-induced currents. For the experiments described here, cells were used 6–10 days following enzyme treatment, a time frame in which the agonist-induced currents are relatively simple. Older cells, in contrast, often show currents with multiple conductance classes and subconductance states.

Acetylcholine (ACh) and carbamylcholine were obtained from Sigma Chemical Co. (St. Louis, MO), and suberyldicholine was generously provided by Dr E. Neher. Agonist-containing solutions were stored as frozen concentrates and diluted into pipette solutions which were filtered (0·2 μm) immediately before use.

Single-channel currents were recorded from membrane patches in the ' cell-attached ' configuration, using standard patch-clamp techniques (Hamill, Marty, Neher, Sakmann & Sigworth, 1981). For all experiments the bath solution contained (mM): KCl, 140; NaCl, 5·4; $CaCl_2$, 1·8; $MgCl_2$, 1·7; adjusted to pH 7·4 with NaOH, 10. Two pipette (extracellular) solutions were used: high-potassium standard solution: KCl, 142; NaCl, 5·4; $CaCl_2$, 1·8; $MgCl_2$, 1·7; HEPES, 9·5; adjusted to pH 7·4 with NaOH, 5. High-potassium low-calcium solution: KCl, 142; NaCl, 5·4; $MgCl_2$, 2·0; EGTA, 1; HEPES, 9·5; adjusted to pH 7·4 with NaOH, 5. Pipettes were fabricated from soft flint glass, coated with Sylgard (Dow–Corning, Midland, MI), and heat-polished and filled with agonist-containing solutions immediately before use. Under these conditions (particularly this enzyme treatment) gigaseals could be formed regularly (30–100 gigohms), and single-channel currents could be recorded for 30–60 min. It was found that a wider voltage range could be applied for prolonged periods using the high-potassium low-calcium solution in the pipette.

These experimental conditions were chosen to optimize the temporal resolution of the data and to provide lengthy recordings containing a large number of events occurring at a low frequency. Initial measurements were obtained at 21 °C with a frequency band width of 3400 Hz and using sodium as the main permeant ion. These preliminary measurements revealed many brief open and closed periods which approached the frequency response limits of the recording system. Subsequently, currents were recorded at low temperature (9–11 °C) to prolong the dwell times, and potassium was substituted for sodium to increase the signal-to-noise ratio ($G_K = 1{\cdot}5\ G_{Na}$). Using the outside-out patch configuration, a band width of 3400 Hz, and a sampling rate of 20 kHz, current pulses as brief as 150 μs were resolved (Sine & Steinbach, 1984*a*). With this improved resolution more brief open and closed times were resolved, but the records were not optimal for several reasons. First, the closed durations were still very brief, with time constants about 50–70 μs. Secondly, an intermediate duration closed state (0·3–1·0 ms) was observed consistently, but was not well defined due to its low rate of occurrence. These limitations are overcome in the present work by recording from cell-attached patches. The cell-attached configuration is advantageous because it yields current recordings with lower noise, enabling a wider band width (7000–8000 filtering and 40 kHz sampling rate) and remains stable for extended periods (30–60 min), permitting the recording of many single-channel events. Under these conditions it is possible to resolve transitions as brief as 100 μs clearly, and to obtain records containing 1000–3000 events.

Single-channel currents were recorded and analysed as described previously (Sine & Steinbach, 1984*a*, 1986). In brief, currents were recorded on FM analog tape (15 in. s^{-1}, Racal Store 4DS, Sarasota, FL) and replayed for analysis. A complete temporal representation was obtained for each experiment using an interrupt-driven sampling program provided by Dr F. J. Sigworth. Analog signals were filtered at 7–8 kHz (8-pole Bessel with cut-off frequencies given as the −3 db point), sampled at intervals of 25 μs, and stored on magnetic disks using a PDP 11/34 computer (Digital Equipment Corp., Waltham, MA). The threshold for current detection was established as halfway

between the mean base line and open-channel currents, and transitions were accepted which crossed threshold for more than three sample points. The raw digitized data were searched for transitions automatically and each detected transition was approved or rejected by the operator. Multiple openings, which were quite rare (< 0·01 of all openings), were counted as such but were not included in further analysis. The reduced data were then stored for further analysis as a series of triplets for each event, consisting of open durations, closed durations and mean current amplitudes.

The reduced data were used to construct open- and closed-duration histograms which are plotted as probability density functions. The histograms were fitted by the sum of exponents by fitting each exponential component sequentially starting from the slowest, using a non-linear least-squares technique (Sine & Steinbach, 1986). Each component was corrected for the distortion due to digitization (see Appendix 1). The time constant is not altered by digitization, but the amplitude is over-estimated when the time constant approaches the sample interval. Therefore, the total number of events is estimated for each component by multiplying the fitted area of the histogram by a factor determined by the time constant for that component (see Appendix 1). For events with a mean duration of 1 ms and a sampling interval of 25 μs, the correction factor is close to 1 (0·99). For events with a mean of 50 μs this factor is significant (0·76).

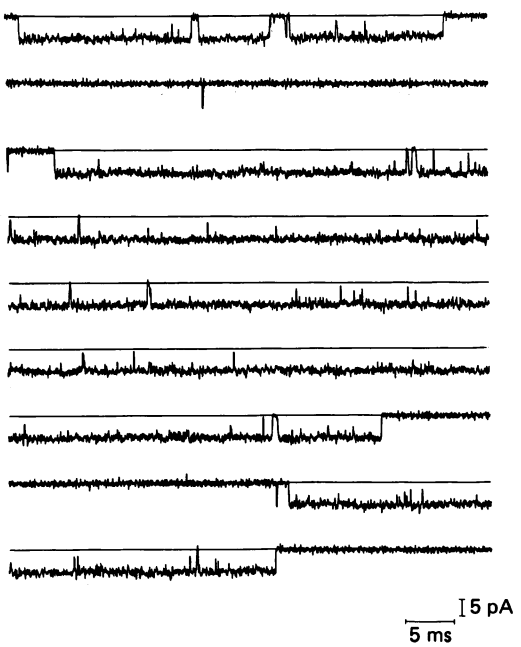

Fig. 1. Single-channel currents recorded from a cell-attached patch in the presence of 100 nM-ACh, with high-potassium normal-calcium buffer in the pipette, at −160 mV and 11 °C. Segments of the current record are shown low-pass filtered at 8000 Hz and sampled at intervals of 25 μs. The horizontal lines indicate the mean base-line current amplitude. The first trace shows a single burst, the second (non-consecutive) trace shows an isolated brief opening. The next five traces show a single long burst. The last two traces show a third burst. Note the absence of sublevels and the presence of very brief closures, long closures and an apparent excess of intermediate-duration closures.

RESULTS

General features of agonist-induced single-channel currents

Fig. 1 illustrates the general features of single-channel currents induced by a low concentration of agonist, 100 nM-ACh. Two distinct types of activity are observed: brief-duration openings which appear as isolated events, and bursts of

several long-duration openings separated by short-duration closed periods. These features are qualitatively similar to those described in other studies of receptor activation. The kinetics of this bursting activity can be analysed to give estimates of the rates for leaving the doubly liganded but closed state of the receptor: the channel opening rate, β, and the agonist dissociation rate k_{-2}, (Colquhoun & Hawkes, 1981).

We use the approach introduced by Colquhoun & Hawkes (1981) (see also Appendix 2) to estimate the rate constants, β and k_{-2}, for the following receptor activation scheme:

$$2A + R \underset{k_{-1}}{\overset{k_1}{\rightleftharpoons}} AR \underset{k_{-2}}{\overset{k_2}{\rightleftharpoons}} A_2R \underset{\alpha}{\overset{\beta}{\rightleftharpoons}} A_2R^*. \qquad \text{scheme (1)}$$

In scheme (1), two agonist molecules (A) combine with the receptor (R) with association rate constants, k_1 and k_2 and dissociate with rates k_{-1} and k_{-2}. The fully occupied receptor (A_2R) adopts the open-channel state (A_2R^*) with forward rate, β, and the open state dissipates with the rate α. At low agonist concentrations the time constant for short-duration closures is $(\beta + k_{-2})^{-1}$ and the number of closures per burst of openings is β/k_{-2} (Colquhoun & Hawkes, 1981). The following sections describe the analysis of burst kinetics and the experiments which associate short-duration closures with particular steps in scheme (1).

Analysis of closed durations

The distribution of closed durations is shown in Fig. 2 for an experiment in which 30 nM-suberyldicholine was applied to a cell-attached patch held at -100 mV. The closed-duration histogram is described by the sum of three exponentials. The major slow component is associated with periods between independent activation episodes. Moreover, two distinct short-duration components are shown on the main panel: a brief-duration component with a time constant of 50 μs, and an intermediate-duration component with a mean of 450 μs. Both brief and intermediate closures were observed consistently for the three agonists examined. Throughout the paper the term ' brief closures ' refers to closures with a time constant of about 50 μs and ' intermediate closures ' to those with a time constant between 300 μs and 1 ms. Brief and intermediate closures, then, emerge as potential dwells in the A_2R state which end by re-entering the A_2R^* state (see scheme (1)). However, at low agonist concentrations scheme (1) predicts that only one brief-duration component will be experimentally resolvable in the closed-time histogram (Colquhoun & Hawkes, 1981). Therefore, it is necessary to determine which class of closings reflects activation processes. After a description of burst durations, the following section presents estimates of β and k_{-2} for both brief and intermediate closures.

Analysis of burst durations

It is necessary to quantify the number of bursts enclosing the short-duration closures in order to estimate β and k_{-2}. Knowing the temporal distribution of short-duration closures, a burst may now be defined as a sequence of openings separated by closed periods shorter than 3 ms. The burst duration, then, is the sum of the closely spaced open periods plus the intervening brief and intermediate closed

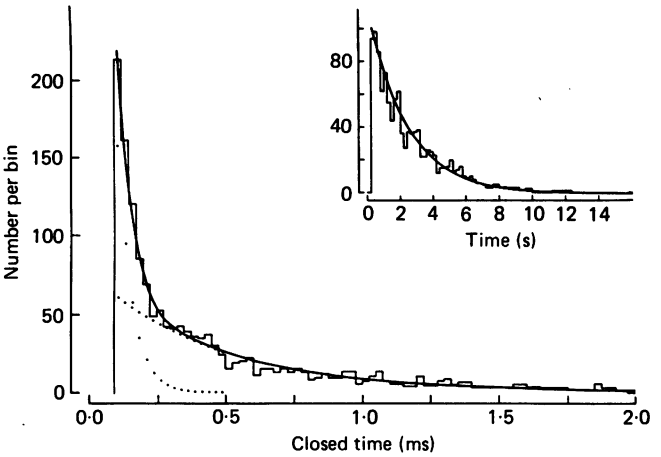

Fig. 2. Closed-duration histogram for currents elicited by 30 nM-suberyldicholine. The histogram is shown on two time scales to illustrate brief (main panel) and long-duration (inset) closures. The histogram is fitted by the sum of three exponentials, shown by the upper continuous curve, with the lower dotted curves showing contributions of brief and intermediate closures. Currents were recorded from a cell-attached patch held at −100 mV, cooled to 11 °C, with high-potassium normal-calcium solution inside the recording pipette. The signal was filtered and sampled as described under Methods. A total of 3167 events were recorded with a record length of 3550 s. The over-all fit contains three components with time constants, t, and a number of events, n, of component 0: $t_0 = 2379$ ms, $n_0 = 1338$; component 1: $t_1 = 449$ μs, $n_1 = 1372$; component 2: $t_2 = 50$ μs, $n_2 = 2293$.

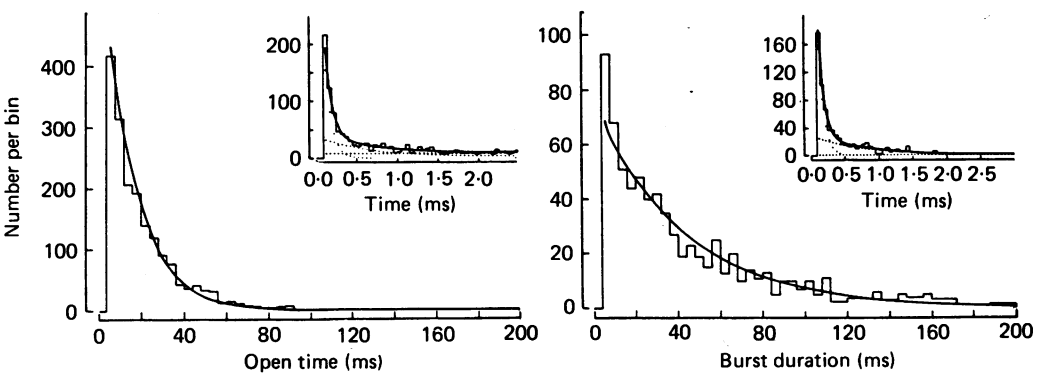

Fig. 3. Histograms of open durations (left panel) and burst durations (right panel). Each histogram is shown on two time scales for long-duration events (main panel) and short-duration events (inset). The histograms are fitted by the sum of three exponentials shown by the continuous curve; the contributions for each component are given by the lower dotted curves. The record is the same one analysed in Fig. 2. Openings were concatenated to form bursts as described in the text, using a maximum intraburst interval of 3 ms. Both histograms are fitted with three components. For bursts: component 0: $t_0 = 42{\cdot}7$ ms, $n_0 = 812$; component 1: $t_1 = 0{\cdot}79$ ms, $n_1 = 447$; component 2: $t_2 = 79$ μs, $n_2 = 997$. For open durations: component 0: $t_0 = 15{\cdot}1$ ms, $n_0 = 2406$; component 1: $t_1 = 0{\cdot}64$ ms, $n_1 = 483$; component 2: $t_2 = 78$ μs, $n_2 = 1005$. Note that the slowest component is prolonged substantially and contains fewer entries in the burst-duration histogram, while components 1 and 2 show little change.

periods. Fig. 3 shows the burst-duration histogram and the corresponding open-duration histogram from the record that is analysed for closed durations in Fig. 2. Both histograms exhibit a major long-duration class of openings (main panel) well separated from two smaller components with short durations (inset). The briefest of these short-duration openings is always observed, with a time constant of 80–200 μs, whereas intermediate-duration openings are evident in about 60 % of the records and are observed more often at relatively hyperpolarized potentials (more negative than -130 mV). The long-duration time constant is prolonged in the burst-duration histogram, whereas there is no change in the properties of either brief or intermediate openings. These results provide evidence that short-duration closures are closely associated primarily with long-duration openings. In later sections this idea is extended to demonstrate that bursts of openings reflect primarily one type of activation process as implied by scheme (1). The number of bursts was estimated from the area of the major slow component of the burst-duration histogram.

To sum up the analysis of Figs. 2 and 3, 812 bursts were observed with 1372 intermediate closures and 2293 brief closures, leading to estimates of 1·69 intermediate closures per burst and 2·82 brief closures per burst. The decay rates are 20000 s^{-1} for the brief component and 2227 s^{-1} for the intermediate component. These parameters lead to quite different estimates for β and k_{-2}. If intermediate closures correspond to closings to the A_2R state followed by reopening to the A_2R^* state, then β is estimated to be 1399 s^{-1} and k_{-2} to be 828 s^{-1}. However, if brief closures reflect closings to the A_2R state, β is estimated to be 14764 s^{-1} and k_{-2} to be 5236 s^{-1}. After a brief consideration of alternative sources of short-duration closures, the following sections describe experiments which identify the closures associated with receptor activation processes.

Alternative processes resulting in brief closures

Potentially, brief- or intermediate-duration closures could result from agonist-induced channel block or from fast desensitization. Although all agonists block the open channel, the dissociation constants for block are relatively high: 2 mM for ACh, 4 mM for carbamylcholine, and 210 μM for suberyldicholine, at -100 mV (Sine & Steinbach, 1984*b*). In the present experiments, agonists were used at the following concentrations: 50–100 nM for ACh, 1–2 μM for carbamylcholine, and 30 to 50 nM for suberyldicholine. At these low concentrations the forward rate for detected blocking events would be low, about 0·1 s^{-1} for ACh, 0·5 s^{-1} for carbamylcholine, and 0·8 s^{-1} for suberyldicholine. These rates are much lower than the observed rates of either brief or intermediate closures (see Table 1, part A). The durations of the blocked state also differ from those seen in these low-concentration closed-time histograms. Channel block, then, is unlikely to generate either brief or intermediate closures.

Desensitization, too, develops at agonist concentrations much higher than those used in these experiments. Tracer ion-flux measurements reveal dissociation constants for desensitization of 500 nM for suberyldicholine and 30 μM for carbamylcholine (Sine & Taylor, 1979, 1980), while single-channel measurements suggest that desensitization is not apparent at concentrations below 1 μM for suberyldicholine, 30 μM for carbamylcholine and 3 μM for ACh (Sine & Steinbach, 1984*a*). Thus the agonist concentrations used are low enough to avoid the complications due to desensitization.

Low agonist concentrations were also chosen to elicit a low frequency of activation episodes and to be within the theoretical low concentration limit for receptor activation. The low concentrations employed elicit openings at a very low frequency, typically 0·3–2 s^{-1}. At these low frequencies, independent openings would very seldom be separated by as little as 3 ms. To meet the low concentration limit, the agonist concentration must be low relative to the dissociation constant for binding to activatable receptors. For the AChR on BC3H–1 cells the concentrations producing 50 % reduction of the initial rate of α-neurotoxin binding are 10^{-4} M for carbamylcholine and 10^{-6} M for suberyldicholine for binding to the low-affinity resting state of the receptor (Sine & Taylor, 1979, 1980). A value of 3×10^{-6} M is estimated for ACh from comparable measurements from *Torpedo* receptors (Quast, Schimerlik, Lee, Witzemann, Blanchard & Raftery, 1978; Cash, Aoshima & Hess, 1981). Desensitization or channel block would result in apparent higher affinity binding of agonist, so the actual dissociation constants are, if anything, larger than these values. These dissociation constants indicate that the agonist occupies less than 1 % of the binding sites at the concentrations used in these experiments. At this low degree of occupancy, predictions from scheme (1) show only one brief closed time component with a time constant of $(\beta + k_{-2})^{-1}$ and a mean number of β/k_{-2} closures per burst (see Appendix 2).

Given the observation of two brief closed-duration components, it is important to identify which of these components is most likely to reflect receptor activation processes. It seems probable that a closed-time component that reflects dwells in A_2R will exhibit agonist specificity in its rate of occurrence (i.e. α), its duration ($(\beta + k_{-2})^{-1}$) and its probability of occurrence ($\beta/(\beta + k_{-2})$). Therefore, the following experiments were designed to determine whether either closed-duration component exhibits agonist specificity in its properties.

Agonist specificity

Single-channel currents were recorded in the presence of low concentrations of acetylcholine, carbamylcholine, and suberyldicholine under identical conditions for each agonist (−100 mV, 11 °C). For each experiment, histograms were constructed of closed durations and burst durations as described for Figs. 2 and 3. The histograms were fitted by the sum of exponentials and the fitted quantities were used to estimate three rate constants shown in scheme (1); β, k_{-2} and α. In addition, the rate of occurrence was calculated for both brief and intermediate closures per second of channel open time.

Table 1 (part A) compares the kinetic properties of bursts of openings for the three agonists. The time constant for intermediate closures differs about two-fold between agonists, whereas the time constant for brief closures is virtually constant. The number of closures per burst varies 7-fold for intermediate closures but only 2-fold for brief closures. The three agonists elicit intermediate closures at different rates during channel openings, while brief closures occur at about the same rate for each agonist. Hence, the measured parameters exhibit greater agonist dependence for intermediate closures than for brief closures.

Table 1 (part B) compares the estimated transition rates for the three agonists. Analysis of intermediate closures yields β estimates differing several-fold among

TABLE 1. Parameters of gaps within bursts and their derived rates

A. Parameters of gaps within bursts

		Intermediate closures				Brief closures		
Agonist	n	t_B (ms)	t_c (μs)	gaps per burst	gaps s^{-1}	t_c (μs)	gaps per burst	gaps s^{-1}
				High-potassium normal-calcium				
ACh	4	49·9±9·4	877±184	0·37±0·11	7·6±2·8	48·3± 7·8	2·28±0·92	48·2±24
		52·7	584	0·39	7·3	44·8	2·73	50·9
Carb.	6	23·5±6·0	1022±336	0·19±0·05	8·7±2·3	49·9±9·3	1·27±0·39	58·6±30
		20·9	872	0·20	8·9	53·1	1·24	54·5
Sub.	2	61±15	484±50	1·72±0·04	31·1±11	49·0±24	2·63±0·29	49·2±24
		52·4	428	1·77	33·3	50·0	2·60	50·0
				High-potassium low-calcium				
ACh	4	26·7±5·9	495±260	0·19±0·06	6·8±0·7	48·9±6·8	1·67±0·67	61·0±11
		29·0	259	0·25	8·2	41·8	2·06	66
Carb.	1	14·4	290	0·086	5·9	44·7	0·92	64

B. Rates derived from gaps within bursts

	Intermediate closures				Brief closures			
Agonist	β s^{-1}	k_{-2} s^{-1}	α s^{-1}	$\frac{\beta}{\beta+\alpha}$	β s^{-1}	k_{-2} s^{-1}	α s^{-1}	$\frac{\beta}{\beta+\alpha}$
				High-potassium normal-calcium				
ACh	321±134	860±144	23·5±6·5	0·93	13904±2790	6500±1541	62±20	0·995
	483	1229	23·8	0·95	16321	5979	72·7	0·995
Carb.	179±89	891±336	58·7±16·9	0·75	11952±2908	8606±1019	87±16	0·993
	190	957	52·3	0·78	10419	8403	97·6	0·991
Sub.	1311±126	765±89	44·1±16·5	0·967	12314±3594	4682±856	61±28	0·995
	1492	843	50·4	0·965	13783	5301	66·4	0·995
				High-potassium low-calcium				
ACh	412±290	2136±1092	46·8±8·4	0·90	12783±3375	7945±1040	97·2±4	0·992
	792	3069	42·8	0·939	16093	7812	104·9	0·993
Carb.	273	3176	79·3	0·78	10714	11646	135	0·987

Two rows of parameters are presented for each agonist ACh,carbamylcholine (Carb.) and suberyldicholine (Sub.). The upper row is the mean (±S.D.) for the data from n patches. The lower row gives values from analysis of a single summed histogram of data from n patches. All data obtained at −100 mV, 11 °C. t_B is the fitted time constant for the slowest component of the burst duration histogram. t_C is the fitted time constant for the specified closed duration component. Gaps per burst is the ratio of the numbers of the specified closures to long duration bursts. Gaps s^{-1} is the ratio of the numbers of the specified closures to the total open time within bursts. β and k_{-2} are the rates derived from the decay rate of the specified closed time component t_c, and the number of gaps per burst. α is the number of closures between bursts plus the number of closures in the specified intraburst component, divided by the total open time.

agonists, whereas the apparent value of β from brief closures is similar for these agonists. Agonist specificity also emerges for the intermediate closures in the calculated equilibrium probability of the open-channel state, $\beta/(\beta+\alpha)$. In accordance with previous findings, carbamylcholine is less effective than ACh at opening the channel, with opening probabilities of 0·77 and 0·93 respectively (Dionne, Steinbach & Stevens, 1978; Adams, 1981). Brief closures, conversely, yield opening probabilities approaching unity for all three agonists. Over-all, these observations suggest that intermediate closures arise through processes of receptor activation because they show greater agonist specificity. Brief closures, in contrast, exhibit properties which appear to be independent of the agonist used to activate the channel. The data suggest that brief closures result from 'flickering' of the open channel to a closed state different from A_2R, whose properties are independent of the agonist and appear to be intrinsic to the open channel *per se*.

Scheme (1) may be expanded to account for both brief and intermediate closures.

$$2A+R \underset{k_{-1}}{\overset{k_1}{\rightleftharpoons}} AR \underset{k_{-2}}{\overset{k_2}{\rightleftharpoons}} A_2R \underset{\alpha}{\overset{\beta}{\rightleftharpoons}} A_2R^* \underset{b}{\overset{f}{\rightleftharpoons}} A_2R'. \qquad \text{scheme (2)}$$

The data suggest that intermediate closures arise through closings to the A_2R state followed by reopening to the A_2R^* state. β is comparable to k_{-2}, so binding is not at equilibrium on the time scale of channel conformational changes. Interestingly, estimates of k_{-2} are similar for the three agonists, suggesting that differences in agonist binding affinity may reside in the association rates, k_1 and k_2, or in k_{-1}. Finally, open channels (A_2R^*) enter a transient closed state, A_2R'. The forward and backward rates, f and b, do not show agonist specificity but represent a reaction intrinsic to open channels.

Voltage dependence of burst kinetics

Several patches were stable enough to permit a detailed analysis of burst kinetics at different membrane potentials. Typical histograms are shown for one patch at two voltages in Fig. 4 to illustrate the qualitative features of voltage dependence. At more negative potentials the duration of bursts increases and there is a substantial rise in the number of both brief and intermediate closures. These findings suggest that the rate constants in scheme (2) change with voltage as described in the following analysis. Patches with high-potassium low-calcium solution in the pipette (extracellular) were stable over a wider range of applied voltages, and so more data were obtained from single patches and over a wider potential range with the low-calcium solution (e.g. Figs. 4–6). Data from a single patch are shown in Figs. 5 and 6. Mean voltage dependences are given in Table 2.

In the analysis of voltage dependence, it is assumed that bursts of openings reflect the activity described by scheme (2). First, the analysis of intermediate closures is described, which appear to be related to the rate constants, β, k_{-2}, and α (Fig. 5). Secondly, the properties of brief closures are examined which correspond to the rates f and b (Fig. 6).

Fig. 5 shows the voltage dependence of the measured parameters of intermediate closures for one patch at five potentials. The number of closures per burst increases e-fold for 69 mV of hyperpolarization, but the mean closed duration is relatively insensitive to potential (e-fold per 313 mV). These findings indicate that β increases

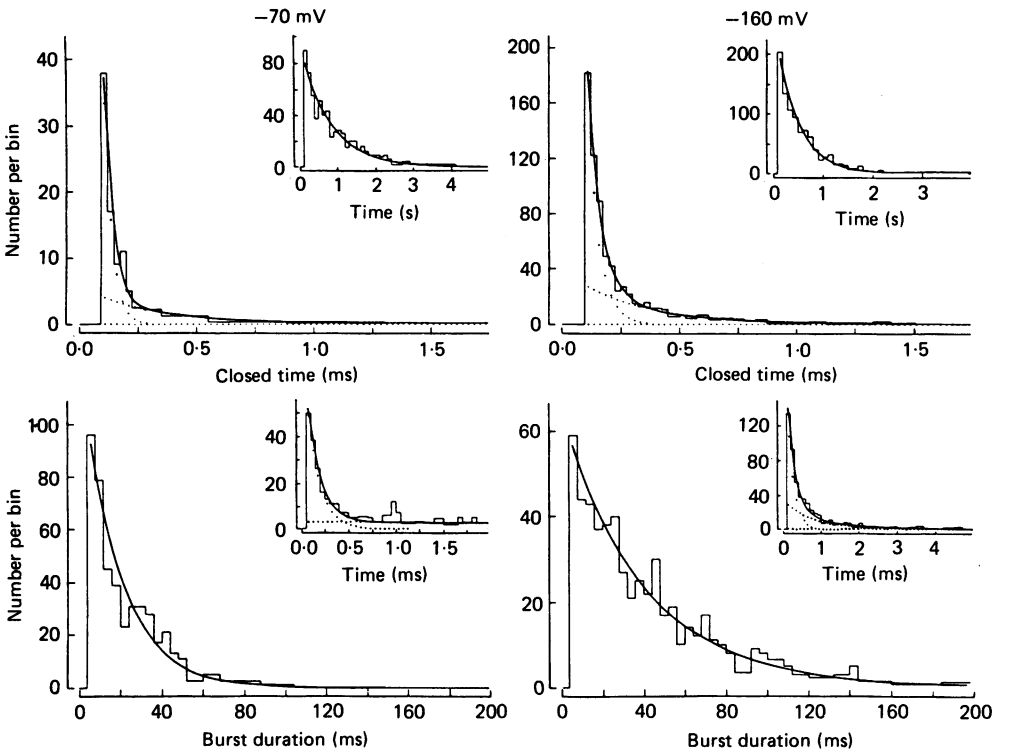

Fig. 4. Voltage dependence of burst kinetics. The top two panels show the closed-duration histograms with brief-duration events on the main panel and long-duration events on the inset. The lower two panels show burst-duration histograms with long-duration events on the main panel and brief-duration events on the inset. Closed-duration and burst-duration histograms are shown for records from the same patch at −70 mV and −160 mV with high-potassium low-calcium buffer solution in the pipette. The top two panels show the closed-duration histograms, and the lower two panels show the burst-duration histograms. Bursts were recognized using a 3 ms maximum intraburst interval. For the −70 mV data, the fitted quantities are: closed durations, component 0: $t_0 = 793$ ms, $n_0 = 766$; component 1: $t_1 = 306\ \mu$s, $n_1 = 67$; component 2: $t_2 = 33\ \mu$s, $n_2 = 1020$. Burst durations, component 0: $t_0 = 18{\cdot}0$ ms, $n_0 = 578$; component 1: $t_1 = 267\ \mu$s, $n_1 = 217$. For the −160 mV data: closed durations, component 0: $t_0 = 466$ ms, $n_0 = 1205$; component 1: $t_1 = 301\ \mu$s, $n_1 = 457$; component 2: $t_2 = 50\ \mu$s, $n_2 = 2237$. Burst durations, component 0: $t_0 = 40{\cdot}5$ ms, $n_0 = 643$; component 1: $t_1 = 0{\cdot}77$ ms, $n_1 = 274$; component 2: $t_2 = 178\ \mu$s, $n_2 = 412$. Note that hyperpolarization results in a substantial increase in the number of brief and intermediate closures, and prolongs the mean burst duration.

with hyperpolarization (e-fold per 120 mV), while k_{-2} shows a weaker and opposite voltage dependence. In terms of scheme (1), the ratio β/k_{-2} increases with hyperpolarization whereas the sum $\beta + k_{-2}$ decreases slightly, since β is smaller than k_{-2}. Similar results were obtained with five other patches, each one at three or more potentials, and with numerous patches at two potentials (see Table 2). In general, β increases with hyperpolarization, whereas k_{-2} shows no clear voltage dependence. Interestingly, k_{-2} is three times larger in the presence of the low-calcium

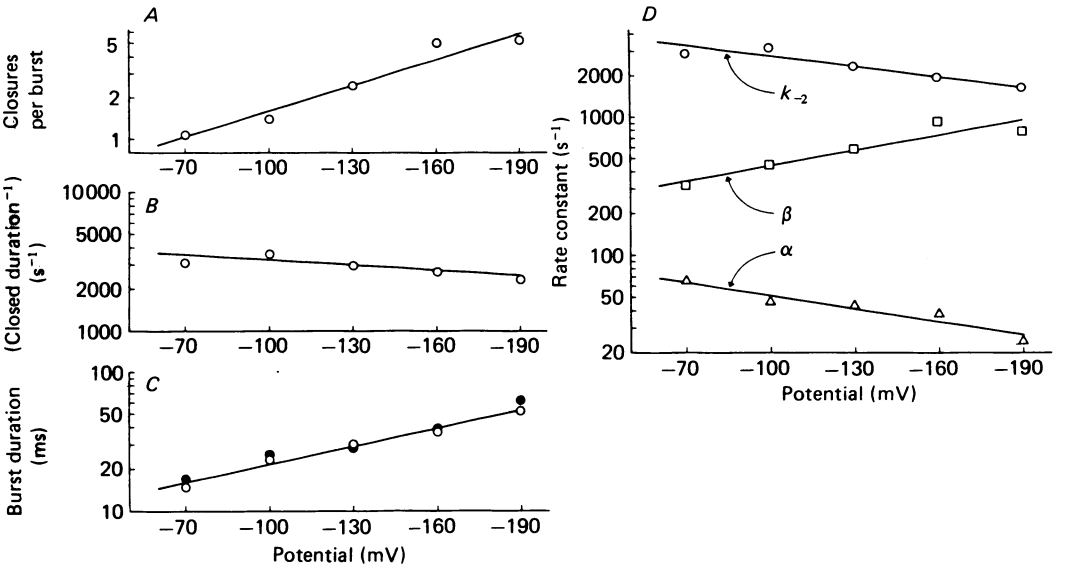

Fig. 5. Voltage dependence of burst kinetics: parameters associated with intermediate closures. Single-channel currents were recorded from one patch (same patch as Fig. 4, high-potassium low-calcium buffer in the pipette) at the indicated potentials. *A*, the mean number of intermediate closures per burst of openings. *B*, the reciprocal time constant for intermediate closures. *C*, the mean burst duration, t_B. Open symbols indicate the reciprocal decay rate of the slow component of the burst duration histogram. Filled symbols give the calculated mean burst duration from the relation: $t_B = 1/\alpha\ (1+\beta/k_{-2})$. *D*, transition rates estimated from intermediate closures. The rates, α (△), β (□), and k_{-2} (○) were calculated as described in Table 1. The lines shown are least-squares fits to the data with the following voltage dependencies (mean values from Table 2 in parentheses): *A*, closures per burst −69 mV (−73); *B*, reciprocal mean intermediate closed duration +313 mV (+1573); *C*, t_B −101 mV (−111); *D*, k_{-2} +164 mV (+1854), β −120 mV (−89), α +139 mV (+158). The voltage dependencies of the mean closed duration and of the estimated k_{-2} were weak and therefore the estimates varied between runs.

TABLE 2. Voltage dependence of burst kinetics

	ACh, normal calcium	ACh, low calcium
Parameter	k (mV)	k (mV)
t_B	−154	−111
Intermediate gaps		
t_c	−131	−1573
gaps per burst	−52	−73
β	−52	−89
k_{-2}	+4990	+1854
α	+154	+158
Brief closures		
t_c	−1069	−459
gaps per burst	−44	−108
gaps s^{-1}	−65	−253

The values given are the exponential coefficients for an assumed relationship $p(V) = p_o \exp(V/k)$. The coefficients were evaluated by fitting a straight line to semilogarithmic plots of the mean parameter values against voltage over the range −70 mV to −190 mV for the low-calcium solution and −70 mV to −160 mV for the normal calcium.

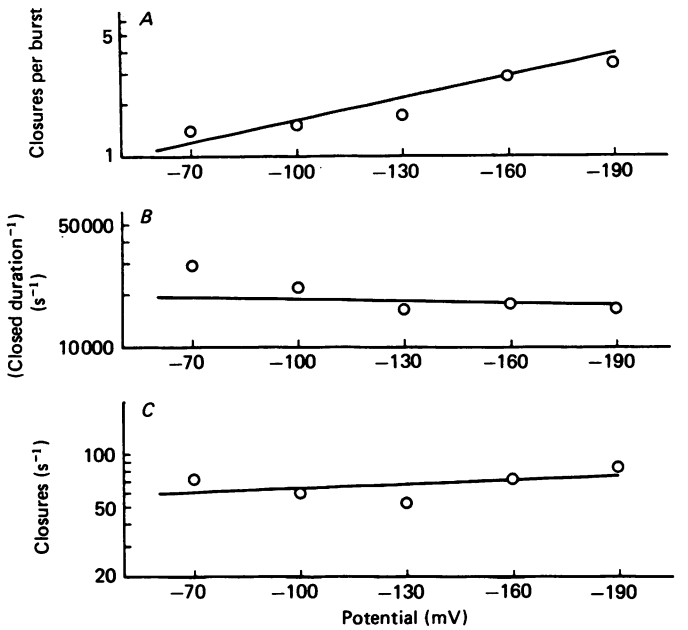

Fig. 6. Voltage dependence of brief closures. Data are from the same patch as Figs. 4 and 5. *A*, the mean number of brief closures per burst. *B*, the reciprocal time constant for brief closures. *C*, brief closures per second of open time, calculated as the ratio of the number of brief closures to the total open time in the record. The lines shown are least squares fits with the following voltage dependencies (with mean values from Table 2 in parentheses): *A*, brief closure per burst −101 mV (−108); *B*; brief closure decay rate +1470 mV (+459); *C*, brief closures/second open time, −558 mV (−253).

buffer. Qualitatively similar observations were made with both carbamylcholine and suberyldicholine, and in the presence of either calcium or magnesium ions externally.

The mean burst duration, t_B, increases e-fold per 101 mV of hyperpolarization, and the channel closing rate, α, is less voltage-sensitive, decreasing e-fold per 130 mV (Fig. 5).

Fig. 6 illustrates the voltage dependence of brief closure characteristics. The number of brief closures per burst increases e-fold for 100 mV of hyperpolarization, approximately in parallel with the increase in the mean burst duration. In contrast, there is only a weak voltage dependence of the frequency of brief closures per second of open time (increasing e-fold for 500 mV of hyperpolarization). However, in the presence of calcium, the frequency of brief closures per second of open time increased with voltage (Table 2), although at −100 mV it did not differ much with either calcium or magnesium externally (Table 1). Finally, the time constant for brief closures is insensitive to potential, decreasing e-fold per 1500 mV of hyperpolarization. Qualitatively similar findings were obtained for the three agonists and in the presence of either calcium or magnesium. Over-all, these observations show that the forward rate, f, may increase with hyperpolarization depending on the presence of calcium, and the backward rate, b, is insensitive to potential.

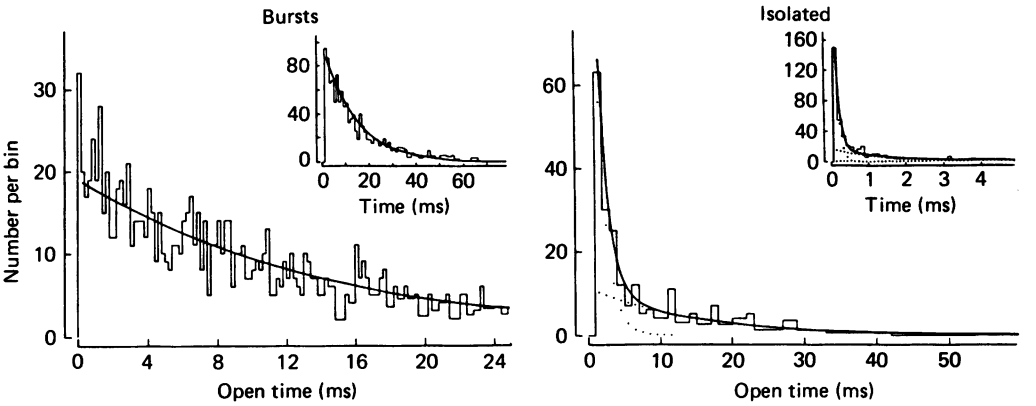

Fig. 7. Sorted open-duration histograms: left panel, openings in bursts; right panel, isolated openings. For bursts, the main panel shows brief open durations and the insert shows long openings. For isolated events, the main panel shows long open durations while the insert shows short-duration openings. The histograms shown are constructed from currents recorded in the presence of 30 nM-suberyldicholine with high-potassium normal-calcium buffer in the pipette, at 11 °C, −100 mV (same patch as Figs. 2 and 3). Openings in bursts were identified using a maximum intraburst interval of 3 ms as described in Fig. 3. For openings in bursts, the data are well described by a single-exponential distribution (continuous curve) with a mean $t_0 = 13{\cdot}9$ ms and $n_0 = 1326$ events. The isolated openings are fitted by the sum of three exponentials (continuous curve) with the components shown by lower dotted curves: component 0: $t_0 = 14{\cdot}5$ ms, $n_0 = 166$; component 1: $t_1 = 1{\cdot}3$ ms, $n_1 = 222$; component 2: $t_2 = 100$ μs, $n_2 = 507$.

Sorted open-duration histograms

Given the occurrence of brief- and long-duration openings, it becomes important to answer two interrelated questions. First, do bursts of openings reflect the activation of a single open state as represented in scheme (2)? Secondly, do some brief- and intermediate-duration closures occur between brief- and long-duration openings? Both questions may be approached by analysing sorted open-duration histograms. To construct the sorted histograms each opening is classified as being either part of a burst, or isolated using 3 ms as the maximum intraburst interval as described in Fig. 3. Examples of sorted open-duration histograms are shown in Fig. 7. For the experiment shown, openings within bursts appear homogeneous, being well described by a single-exponential distribution. In other experiments, however, some brief-duration bins deviate slightly above the curve of a single exponential, apparently representing occasional brief openings coupled to long openings. This small brief-duration component becomes more pronounced at more hyperpolarized potentials (negative to −130 mV), but still accounts for only 3–5% of the total detected openings within bursts. These results show that long-duration openings represent the vast majority of openings within bursts, but on occasion the receptor may adopt the brief open state. Also, at least 95% of the detected brief and intermediate closures occur between long-duration openings, with only a few of these closed dwells occurring between brief and long openings.

The histogram of isolated open durations is described by the sum of three exponentials (Fig. 7). The slowest component corresponds to solitary long-duration

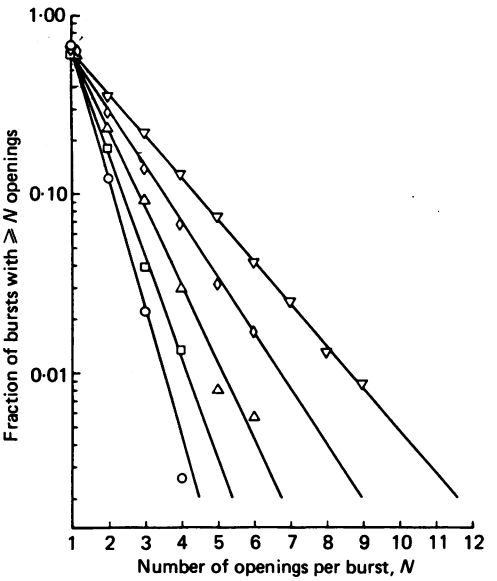

Fig. 8. The distribution of bursts with N or more openings. Bursts were identified using a maximum intraburst interval of 3 ms (see Fig. 3), and the number of resolved openings were counted in each burst. In this plot, all bursts contain at least one opening (by definition) and so the total fraction of bursts with one or more openings (ordinate) is 1·00. The symbols on the ordinate give the fraction of resolved long openings (for this experiment, about 0·6). The distribution is shown for the same patch analysed in Figs. 4–6 for the following potentials: −70 mV (○), −100 mV (□), −130 mV (△), −160 mV (◇), −190 mV (▽). The lines through the points show a linear least-squares fit for bursts containing more than one opening. Note that the data are well described by a single geometric distribution for bursts with multiple openings, but that single-event bursts are found in excess. The symbols at the y-intercept (one opening per burst) show the measured fraction of long-duration openings obtained from the area of the slow component of the open-duration histogram. These points lie on the lines, so the excess of single events is due to isolated short-duration openings. In this experiment there is no change with potential in the fraction of long-duration openings. In some experiments, however, that fraction decreased somewhat with hyperpolarization.

openings, as its time constant closely matches the duration of openings within bursts. The remaining isolated components are due to brief and intermediate openings. The histogram of isolated openings, then, supports the idea that brief- and intermediate-duration openings occur primarily outside bursts at low agonist concentrations.

Are bursts homogeneous?

Although bursts consist of predominantly long-duration openings it is possible that several types of bursts occur with different properties. Several tests were applied to look for signs of burst non-homogeneity. For example, the mean open times within bursts were examined and found to be indistinguishable from the mean duration of isolated long openings (see Fig. 7). The mean open time was also found to be independent of the position of an opening within a multi-opening burst. Finally, the mean open time was independent of the number of openings in a burst. The following paragraphs describe three more tests of homogeneity which examine closures within bursts.

The first analysis simply counts the number of bursts with one, two, ..., N openings, and plots the fraction of bursts with N or more openings against N. Fig. 8 shows such a plot for one patch held at five different potentials. The exponential decay after the first point shows that the data are described by a geometric distribution, implying that bursting behaviour is homogeneous. Hence, for all bursts the probability is constant that a closed period is within a burst. This probability, that a closed period is both seen and within a burst, is e raised to the slope of the lines on the semilogarithmic plots. The slopes decrease with hyperpolarization (reopening probabilities increase) as expected, since the numbers of both brief and intermediate closures per burst increase with hyperpolarization. The linear fit describes the data for bursts with two or more openings, because isolated short-duration openings occur in excess. However, the lines fitted to bursts do pass through the point representing all seen long-duration openings, so that isolated long-duration openings also show the same bursting behaviour. All of the data sets obtained conformed to this pattern.

The second test determined whether sequential pairs of closures were correlated in their duration, addressing the question of whether brief or intermediate closures appear as clusters. The approach was similar to that taken by Jackson, Wong, Morris, Christian & Lecar (1983) to examine correlations between brief and long open states. Any closure longer than 3 ms was classified as ' between bursts '. Closures shorter than 3 ms were classified as ' brief ' or ' intermediate ', using a discriminator time chosen to provide approximately equal numbers of resolved brief and intermediate closures (usually brief closures had durations 0·1 ms $\leqslant d <$ 0·175 ms, intermediate closures 0·175 ms $\leqslant d$ 3 ms). Each sequential pair of closures within a burst was classified as brief–brief, mixed or intermediate–intermediate, for the entire record. The predicted numbers of pairs were calculated from the total number of pairs seen, and from the over-all probabilities that resolved closures were classified as brief or intermediate. The observed and predicted numbers were then compared using the χ^2 test. In twenty-three out of twenty-four records the observed and predicted numbers agreed closely, with only one record showing a significant difference from the theory ($P < 0{\cdot}05$). Therefore, brief or intermediate closures do not appear in pairs, preferentially.

The third test examined whether two types of bursts existed, one enriched in brief, and the other in intermediate closures. Closures were classified as described above, and the number of bursts were counted with zero, one, two... brief closures, given that the burst had at least one closure. The numbers of bursts with N brief closures can be predicted if two probabilities are known: the probability that a closing is classified as brief given that it is both seen and identified within a burst, and the probability that a closure is within a burst. These probabilities were calculated from the data and used to predict the expected distribution of bursts with N brief closures, under the null hypothesis that brief and intermediate closures occur in all bursts with constant probabilities. Observed and expected numbers of bursts were compared using the χ^2 test. Twenty-four records were analysed, and in only one case did the observed and predicted numbers differ substantially ($P < 0{\cdot}05$). (This was not the data set which showed possible clustering of closed periods.)

Over-all, bursts appear homogeneous, although both the resolved open-time and closed-time histograms are described by the sums of several exponentials. The probability of reopening (or the probability that a seen closure will be classified as

within a burst) is constant across bursts. Brief or intermediate closures do not occur in sequential pairs, and the numbers of brief closures in bursts can be predicted from the over-all probability that resolved closures are classified as brief duration. These results imply that bursts are produced by a homogeneous population of receptors, which also apparently give rise to isolated resolved-long duration openings.

The predicted numbers of bursts with N resolved brief closures were derived using two probabilities.

$$\pi_0 = \text{prob}\,[\text{closure resolved and called within a burst}],$$
$$\pi_1 = \text{prob}\,[\text{closure called brief}|\text{resolved and called within a burst}].$$

Define

$$Z_1(N) = \text{prob}\,[\text{a burst contains } N \text{ resolved brief closings}].$$

This was evaluated from the sum

$$Z_1(N) = \sum_{M=0}^{\infty} \text{prob}\,[N \text{ resolved brief closings in a burst}|\text{burst contains } M \text{ resolved closings}] \times \text{prob}\,[\text{burst contains } M \text{ resolved closings}]$$

$$= \sum_{M=0}^{\infty} \pi_1^N (1-\pi_1)^{M-N} M!/(N!(M-N)!)\,\pi_0^M \quad (1-\pi_0)$$

$$= \left[\frac{\pi_0\pi_1}{1-\pi_0(1-\pi_1)}\right]^N \left[\frac{1-\pi_0}{1-\pi_0(1-\pi_1)}\right].$$

However, an additional condition was imposed because of the observed excess of isolated shorter duration openings: a burst had to contain at least one resolved intra-burst closing.

$$Z(N) = \text{prob}\,[N \text{ resolved brief closings in a burst}|\text{at least one resolved closing}].$$

If at least one brief closing is detected,

$$Z(N) = Z_1(N)/\text{prob}\,[\text{burst has at least one resolved closing}]; \quad N \geqslant 1.$$
$$= Z_1(N)/\pi_0$$

When no brief closings are detected,

$$Z(0) = \frac{(1-\pi_0)(1-\pi_1)}{(1-\pi_0(1-\pi_1))}$$

π_0 was evaluated from the distribution of bursts with M total closings (e.g. Fig. 8), from the common ratio and from the mean number of seen gaps per burst. If k = semilog regression slope of a plot similar to those in Fig. 8, and M = mean number of resolved gaps per burst for bursts containing at least one gap, $\pi_0 = \exp(k) = (M-1)/M$. These two estimates agreed within 10% on a given data set; the mean value was used in calculations. π_1 was estimated simply as (number of resolved brief closings)/(number of resolved brief and intermediate closings) in the entire record.

Some uncertainty is introduced because the actual calculations are performed using

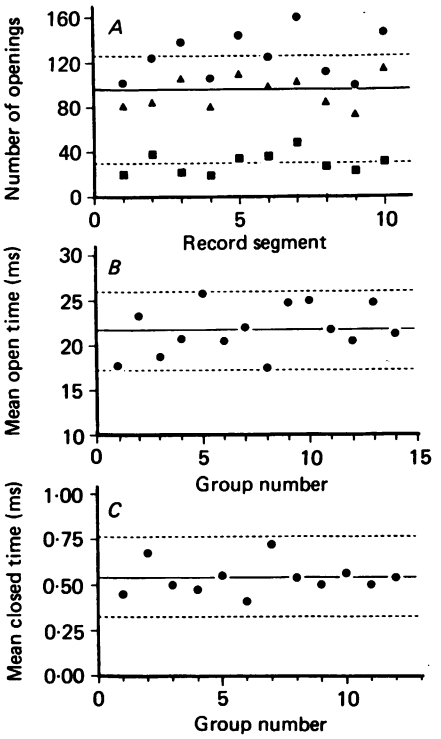

Fig. 9. Stationarity of the data. This Figure shows experimental values as a function of time during the record. *A* shows the opening frequency, *B* shows the mean long-duration open time, and *C* shows the mean intermediate closed time. In *A* the record was divided into ten equal time segments and the number of openings were counted in each segment: ●, total openings; ▲, long-duration openings; ■, brief-duration openings. The discriminator time for classifying brief and long openings was established as the time at which brief and long probability density functions are equal (for this record 0·65 ms). In *B* the mean long-duration open time was computed for consecutive groups of twenty-four openings longer than the discriminator time. The over-all mean open duration is shown by the continuous line, and the points distribute within the limits defined by the dotted lines ($\pm 2 \times$ S.D.$/\sqrt{N}$, 95% limits). In *C* the mean intermediate closed time was computed for closures lasting between 0·2 and 3 ms, and the mean was calculated for groups of twenty-four consecutive dwells. Again the durations distribute about the mean (continuous line) within the boundaries of the dotted lines ($\pm 2 \times$ S.D.$/\sqrt{N}$).

resolved durations. As discussed in Appendix 1, digitization will affect the apparent numbers of detected dwells in various duration classes, and the problems of missed and misclassified dwells are appreciable. For these reasons, relatively weak coupling between closures of a given type might be missed using these tests.

Are the records stationary?

The analysis of scheme (2) requires not only that bursts of openings are homogeneous, but that the rate constants are stationary throughout the record. Several analyses were designed to test the stationarity of each record, First, the record was divided into equal time intervals and the number of brief- and long-duration openings were counted in each interval. Secondly, the mean open and closed times were computed

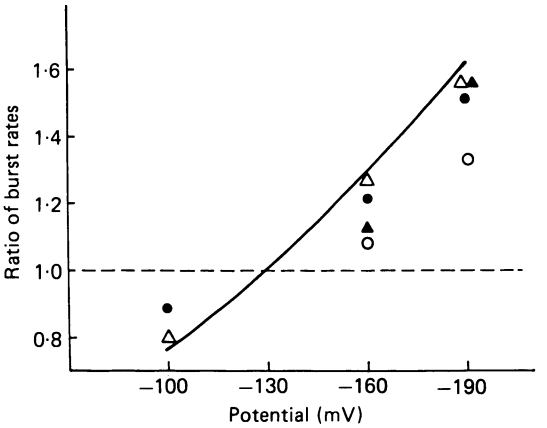

Fig. 10. Burst frequency as a function of potential. Data are shown for four patches (different symbols) in low calcium solution, normalized to the frequency at −130 mV. The burst frequency was obtained from the number of entries in the slow component of the burst-duration histogram divided by the total record length. The line shows the voltage dependence of the ratio $\beta/(\beta+k_{-2})$ using the mean values for β and k_{-2} at −100 (Table 1, part B), a voltage dependence for β of e-fold per 90 mV (Table 2) and neglecting the weak voltage dependence of k_{-2}. The burst frequency increases approximately exponentially with hyperpolarization, e-fold per 160 mV.

for consecutive record segments and compared with the over-all mean dwell times. Fig. 9 is an example of such a stationarity analysis. Brief- and long-duration openings are observed at a relatively constant rate across the record. The Figure also shows the mean duration of long openings and of intermediate closures, which appear to be associated with the reaction steps, β, k_{-2} and α. The segment dwell times fluctuate about the over-all mean values within the boundaries expected for sampling from a single population with an exponential distribution ($\pm 95\%$ confidence levels). Similar results were obtained for the records at four other potentials from the same patch. Over-all, there was no evidence for a time-dependent change of any of the parameters examined. It is concluded that the kinetics of receptor activation are stationary throughout the record.

Burst frequency

The rate of occurrence of bursts is predicted to be $N\beta k_1 k_2/(k_{-1}(k_{-2}+\beta))$, as derived in Appendix 2 (see A2.8), where N is the number of receptors in the patch and the forward binding rates contain the agonist concentration. Qualitatively, this relationship suggests that the burst frequency should increase with hyperpolarization due to the voltage dependence of $\beta/(\beta+k_{-2})$, as we see (see also Redmann, Adams & Clark, 1982; Morris, Wong, Jackson & Lecar, 1983). The voltage dependence of $\beta/(\beta+k_{-2})$ was calculated from the mean parameters for ACh in low-calcium solution, where the most complete sets of data were obtained on single patches. The predicted and observed voltage dependences for the burst frequency are shown in Fig. 10. The predicted voltage dependence is somewhat steeper than that actually seen, but is in fairly good agreement with the data. If genuine, the difference may indicate some voltage dependence in the ratio $k_1 k_2/k_{-1}$.

DISCUSSION

The experiments described examine activation of the AChR by low concentrations of the strong agonists ACh, carbamylcholine and suberyldicholine. Each agonist causes the AChR channel to activate in burst-like episodes consisting of several openings separated by brief closed periods. Kinetic analysis reveals that bursts originate from receptors which adopt primarily one open state, but which can close to two separate closed states. Kinetic properties were compared for three agonists in order to clarify the nature of the two closed states identified as brief closures (mean of 50 μs) and intermediate closures (mean between 300 μs and 1 ms). Intermediate closures exhibit more agonist specificity than brief closures, suggesting that they arise through the receptor activation steps β and k_{-2}. The channel closing rate, α, then may be estimated from the mean burst duration and the number of intermediate closures per burst. For the three agonists, β ranges between 150 s and 1200 s^{-1}, α is between 20 s and 50 s^{-1} and k_{-2} is about 900 s^{-1}.

Channel opening occurs at about the same rate as agonist dissociation, so agonist binding is not at equilibrium on the time scale of channel opening. Channel closing is slower, so the equilibrium probability of being open, $\beta/(\beta+\alpha)$, is quite high and depends on the agonist. The open probabilities are 0·77 for carbamylcholine and 0·93 for ACh, in reasonable accord with estimates from macroscopic current measurements (Dionne *et al.* 1978; Adams, 1981). Both β and α depend on potential, β increasing with hyperpolarization and α decreasing. Agonist dissociation shows little dependence on potential.

The mean burst duration, t_B, increases e-fold for about 110 mV of hyperpolarization. Most of the voltage dependence of t_B arises from the voltage dependence of α, the channel closing rate. The remainder of the voltage dependence comes from the ratio $\beta/(\beta+k_{-2})$, which shows an opposite voltage dependence to α. The estimated voltage dependence for β is higher than that obtained from macroscopic current measurements (Dionne & Stevens, 1975; Neher & Sakmann, 1975) or from single-channel measurements at frog junctions (Colquhoun & Sakmann, 1985), but is comparable to the results from single-channel measurements at snake neuromuscular junctions (Leibowitz & Dionne, 1984). Agonist dissociation has a negligible voltage dependence in the present data. Leibowitz & Dionne (1984) report that k_{-2} increases with hyperpolarization, e-fold per 105 mV, whereas Colquhoun & Sakmann (1985) report little voltage dependence. There is no evidence on the voltage dependence of agonist binding, but the ability of (+)-tubocurarine to inhibit competitively receptor activation at frog end-plates is independent of potential (Colquhoun, Dreyer & Sheridan, 1979).

In contrast to intermediate closures, brief closures show little agonist specificity, and apparently reflect properties of open channels which are independent of the nature of the agonist. The brief closure, then, may be described as the transition of open channels to an endogenous closed state with a forward rate, f, and backward rate, b.

In addition to the present observations at low agonist concentrations, there are further indications that brief closures do not reflect the receptor activation steps, β and k_{-2} in BC3H–1 cells. In particular, the antagonist, (+)-dimethyltubocurarine

(DMT) elicits channel openings with intervening brief closures which decay with a time constant of about 50 μs (Sine & Steinbach, 1986). Kinetic analysis leads to an estimate for β of 6000 s^{-1}, which is inconsistent with the low efficacy of DMT relative to ACh. Over-all, brief closures observed for BC3H–1 receptors do not show the properties expected for receptor activation processes. Instead, brief closures are independent of the nature of the agonist and its concentration, but exhibit characteristics of an intrinsic closed state closely coupled to open channels.

The present interpretation of the closed-duration histograms and the estimated transition rates agree qualitatively with other findings. Carbamylcholine is a weaker agonist than ACh as it shows a lower opening rate (β), a lower probability of opening from the doubly liganded state ($\beta/(\beta+k_{-2})$), and a lower probability of being open ($\beta/(\beta+\alpha)$). Data obtained at high concentrations of ACh and carbamylcholine yield estimates for β which are close to the β estimates from the present low concentration data (S. M. Sine & J. H. Steinbach, in preparation). It is interesting that k_{-2} is so similar for ACh, carbamylcholine and suberyldicholine.

DMT shows a small but reproducible intermediate-duration closed-time component (Sine & Steinbach, 1986). Analysis of this component gives somewhat more reasonable estimates for β and k_{-2} than does analysis of brief closures (β in the range 30–100 s^{-1}, k_{-2} about 900 s^{-1} at -100 mV and 11 °C). However, when these estimates are used to predict the burst frequency, using dissociation constants from flux and binding measurements (Sine & Taylor, 1981), a rather high frequency is calculated (0·2–1 burst s^{-1} $receptor^{-1}$) compared to the observed frequency of 0·1–1 s^{-1} in different patches, especially since the patches contain many receptors (see below). Various mechanisms which could reduce the observed frequency (e.g. channel block) are discussed by Sine & Steinbach (1986). These mechanisms were considered unlikely to produce the reduction of about 10000-fold necessary for the rates estimated from brief closures seen with DMT to be consistent with the observed low frequency of bursts. Even with the rates calculated from intermediate closures seen with DMT the majority of receptors would have to be inactive. Over-all, the data obtained with DMT are certainly more consistent with the present interpretation of the closed-time histograms than with the idea that brief closures reflect reopenings from A_2R, but there are some significant quantitative discrepancies.

A low external calcium concentration was used in some experiments for two reasons. First, calcium was reduced to determine whether brief closures result from calcium ion block of the channel. No such blocking action was apparent in the data. Secondly, measurements of agonist binding and tracer ion flux had suggested that replacement of calcium by magnesium reduced the binding affinity of the agonist by 2–3-fold (S. M. Sine, unpublished observations). The present data indicate that k_{-2} increases when magnesium replaces calcium, which is consistent with a reduced agonist binding affinity.

The number of receptors in a patch may be calculated from the observed frequency of bursts using eqn. (A 2.8) (see Appendix 2),

$$N = (\text{burst frequency})\ (k_{-1}(k_{-2}+\beta))/(\beta k_1\ k_2).$$

The concentration dependence of single-channel kinetics (S. M. Sine & J. H. Steinbach, in preparation) provides estimated dissociation constants suggesting that some

positive co-operativity in binding exists. With ACh, the dissociation constant with one agonist bound is $K_{D,1} \cong 60\ \mu M$, for the second is $K_{D,2} \cong 6\ \mu M$. The values for carbamylcholine are less certain, but are about $K_{D,1} \cong 1000\ \mu M$ and $K_{D,2} \cong 100\ \mu M$. There are no high concentration data with suberyldicholine, but it is assumed to have a slightly higher affinity than does ACh: $K_{D,1} \cong 30\ \mu M$ and $K_{D,2} \cong 3\ \mu M$. These estimates, combined with the present data on β and k_{-2}, allow calculation of N from the burst frequency. With ACh the mean value of N was 47 receptors per patch (eight patches, range 19–96), with carbamylcholine $N = 89$ (seven patches, range 24–139) and with suberyldicholine $N = 58$ (three patches, range 21–77), all at -100 or -130 mV in normal calcium solution. The estimated N was larger for ACh in low calcium solution, $N = 184$ (four patches, 91–302), possibly because it was simply assumed that both k_{-2} and k_{-1} were similarly altered and that neither k_1 nor k_2 changed. These estimates of N are remarkably close to those expected from measurements of α-neurotoxin binding (50–200 receptors μm^{-2}) (Patrick, McMillan, Wolfson & O'Brien, 1977). The pipettes used had resistances of 4–6 MΩ, so the expected patch area is 1–2 μm^2 (Sakmann & Neher, 1983), which would then contain about 100 receptors.

Previous studies on BC3H–1 cells facilitate the design and interpretation of the present experiments. The theoretical low concentration limit is well defined for these ACh receptors by measurements of agonist binding and agonist-induced sodium influx for both carbamylcholine and suberyldicholine (Sine & Taylor, 1979, 1980). Although similar measurements are not available for ACh, it is known that ACh has a slightly lower affinity than suberyldicholine for *Torpedo* ACh receptors (Weiland & Taylor, 1979). Thus, by knowing the binding affinity of suberyldicholine for BC3H–1 ACh receptors, the low concentration for ACh is established. In addition, the properties of agonist-induced channel block for BC3H–1 AChRs have been described, which show that block is not responsible for the observed closed states (Sine & Steinbach, 1984*b*). Finally, the measurements described were obtained on cells at relatively early stages of culture where the receptors exhibit simple kinetic properties. Receptors of BC3H–1 cells, therefore, have been well characterized.

Earlier, results were obtained using outside-out patches from BC3H–1 cells, but with lower temporal resolution (Sine & Steinbach, 1984*a*). The outside-out patch results are qualitatively identical to those obtained with on-cell records, but show some quantitative differences. The mean burst durations in outside-out patches are shorter than those in cell-attached patches (see also Trautmann & Siegelbaum, 1983), and the rate of occurrence of brief closures (f) also is less in outside-out patches. The intermediate duration closed-time component was too small to be analysed in the outside-out patch data, as fewer events were collected in those experiments.

Colquhoun & Sakmann (1981, 1985) examined the activation of single AChR channels at frog junctional regions and described results qualitatively similar to those reported here. Currents were recorded at low temperature (9–11 °C) and current pulses were resolved as brief as 30 μs from high-quality current records fitted to the response characteristics of the recording system. They, too, observed bursts of openings with intervening brief closures and intermediate closures. Intermediate closures appear to be less frequent for the frog receptors and analysis of intermediate closures gives values of β and k_{-2} which are too small to account for data at higher agonist

concentrations. The rates β and k_{-2} were estimated from brief closures for four agonists and show agonist specificity. Suberyldicholine gives an estimate for β of 18000 s^{-1} and for k_{-2} of 2400; for ACh the values are 30000 s^{-1} and 8200 s^{-1} respectively. These rates are similar to the estimates obtained from the present data if brief closures were interpreted as reflecting closures to the A_2R state. Brief closures, however, show differences between BC3H–1 and frog junctional receptors. In the frog, brief closures occur at a 10-fold higher rate, show more agonist specificity, and exhibit a different dependence on voltage (Colquhoun & Sakmann, 1985). Such differences in properties of brief closures may indicate that although the data from frog junctional and BC3H–1 receptors are qualitatively similar, similar closed-duration components may reflect different processes in the two systems.

Dionne & Leibowitz analysed the activation of single AChR channels at snake neuromuscular junctions at a temperature of 21 °C and with a recording band width of 2·5 kHz (Dionne & Leibowitz, 1982; Leibowitz & Dionne, 1984). They observe only one brief closed time component with ACh, and obtain estimates of β and k_{-2} similar to ours when corrected for temperature. In addition, the brief closures show some qualitative features of agonist specificity, being so rare with carbamylcholine that it was not possible to estimate the decay rate of the brief closures. In agreement with our results, β increases and α decreases with hyperpolarization, resulting in an increased opening probability at more negative potentials. However, their estimates for k_{-2} increase fairly steeply with hyperpolarization. As is observed for frog junctional receptors, α is 10-fold greater for snake ACh receptors than is observed for BC3H–1 receptors. In general, activation of snake ACh receptors appears similar to the present observations with BC3H–1 cells. However, it remains to be demonstrated that the closed states analysed in the snake system are associated with receptor activation processes.

Auerbach & Sachs (1984) examined the activation of single AChR channels in cultured chick pectoral muscle at a temperature of 23 °C and a recording band width of 5 kHz. They observe burst-like episodes at low agonist concentrations and detect the occurrence of three separate short-duration closures. One of these closed states has been examined in detail and reflects the entry to a subconductance state with a mean duration of 0·5–1·0 ms. Although such a substate clearly does not reflect the rates β and k_{-2}, it does exhibit agonist specificity in its duration. Two other closed states are observed, with time constants of 0·1 ms and 2–10 ms. These closed states have not been examined in detail. It is not known which closed state reflects receptor activation processes in the chick system.

Receptors on other mammalian muscles have not been examined as extensively as ACh receptors of the frog, snake, or chick. The AChR on young BC3H–1 cells appears similar to non-junctional receptors in adult muscle fibres or cultured myotubes in terms of basic receptor properties such as mean burst duration and single-channel conductance (Brenner & Sakmann, 1983; Siegelbaum, Trautmann & Koenig, 1984). Also, the present estimates of β and k_{-2} are probably lower than those for junctional receptors, as their sum is too small to account for the rate of rise of miniature end-plate currents (m.e.p.c.s). If ACh release and binding were instantaneous, the rate constant for the rising phase of m.e.p.c., or the decay of the m.e.p.c. driving function, should approach $(\beta + k_{-2})$. Hence, the experimentally measured rate

of rise represents a minimal estimate for $(\beta + k_{-2})$. At 23 °C, the driving function decay rate is about 8000 s^{-1} (Linder, Pennefather & Quastel, 1984), whereas the present data indicate that $(\beta + k_{-2})$ approaches 4000 s^{-1}, assuming a Q_{10} of about 3. The decay of the driving function exhibits a weaker voltage dependence than the present estimate of $(\beta + k_{-2})$, but changes with voltage in the same direction.

Scheme (2) describes the activation of bursts of channel openings, which accounts for the majority of the current flow induced by agonists (> 99 %). However, scheme (2) does not account for the occurrence of short-duration openings. The situation is complicated further by the observation of two classes of short-duration openings: brief (100 μs) and intermediate (1 ms). Each duration class of opening has the same conductance, and they are detected only in the presence of agonist. These findings suggest that one receptor population gives rise to all types of opening.

Intermediate-duration openings are clearly apparent at relatively hyperpolarized potentials and when the histograms contain many openings, which accounts for their being overlooked earlier (Sine & Steinbach, 1984*a*). Contrary to the infrequent but detectable close coupling between brief- and long-duration openings, intermediate-duration openings always appear in isolation at all agonist concentrations and membrane potentials. Therefore, we cannot be sure that intermediate openings are produced by the same receptor that generates brief- and long-duration openings.

Brief-duration openings, on the other hand, arise from the same receptor population that elicits long-duration openings. Brief- and long-duration openings exhibit a temporal association at high agonist concentrations, indicating that a single receptor may adopt either open state (Sine & Steinbach, 1984*a*). Even at low agonist concentrations, the present data reveal a small excess of brief events within bursts at very negative membrane potentials. Such coupling within bursts also suggests that the same receptor may take on both brief- and long-duration open states.

Brief-duration openings are most likely to arise from receptors with two bound agonist molecules. The relative frequency of brief and long openings shows little change with agonist concentration for strong agonists, suggesting that brief openings do not originate from mono-liganded receptors (Sine & Steinbach, 1984*a*). Moreover, brief openings are not detected when only one site is occupied by the site-selective weak agonist DMT. Instead, both brief and long openings appear when DMT occupies both high- and low-affinity sites, and their relative frequency is constant over an 80-fold concentration range of DMT (Sine & Steinbach, 1986). Thus, we have not found any evidence that brief-duration openings arise from mono-liganded receptors. Rather, brief and long openings appear to originate from doubly liganded receptors.

It is not known how brief- and long-duration openings are coupled. However, the two open states do not appear to share a common closed state, since different distributions are observed for the closed periods bounding brief and long openings (as implied by the observation that most brief openings occur outside bursts). Hence scheme (2) must be expanded to account for two separate open states and an additional closed state:

$$2A + R \underset{k_{-1}}{\overset{k_1}{\rightleftharpoons}} A + AR \underbrace{\underset{k_{-2}}{\overset{k_2}{\rightleftharpoons}} A_2R \underset{\alpha}{\overset{\beta}{\rightleftharpoons}} A_2R^*}_{\underset{\alpha'}{\overset{\beta'}{\rightleftharpoons}} A_2Q^*} \underset{b}{\overset{f}{\rightleftharpoons}} A_2R'. \qquad \text{scheme (3)}$$

In scheme (3), fully occupied receptors may adopt the Q state (A_2Q) and give rise to short-duration openings (A_2Q^*) with the opening rate β' and closing rate α'. The brace indicates that it is not known how the Q state is coupled to the R state.

In summary, multiple-exponential components are apparent in both the closed-duration and open-duration histograms at low agonist concentrations. Components of the closed-duration histogram appear to be associated with particular states in a receptor activation scheme (scheme (2)), based on the analysis of currents elicited by three strong agonists (ACh, carbamylcholine and suberyldicholine) and one weak agonist (DMT) (Sine & Steinbach, 1986). The association between closed dwell times and receptor states leads to estimates of the rate constants for steps in scheme (2). The estimated rates make predictions for the concentration dependence of receptor activation (S. M. Sine & J. H. Steinbach, in preparation). Although several open duration components are observed, most of the current passed by active AChR channels flows during long-duration openings, whose activity may be described by scheme (2). However, it is not known how either brief or intermediate openings are linked to the long-duration open state. These complications aside, evidence is presented for interpreting components in duration histograms in terms of a particular reaction scheme and for extracting estimates for transition rates in this scheme. The scheme presented is very similar to those used in analysing macroscopic currents through AChR ensembles.

APPENDIX 1

The effect of digitization on apparent dwell times

A digitized record approximates a continuous process, and the uncertainty caused by digitization increases as the continuous process becomes rapid compared to the digitization interval. Since some of the mean dwell times seen in our data approach the digitization interval, a first-order correction is applied, derived as follows.

1.A. Perfect records. The simplest case is a record obtained without noise and with an instantaneous system response. There is only a single-amplitude class of events, and the event detection ' threshold ' is set at the half-maximal event amplitude. The duration of a dwell is defined as the number of sample intervals between the first data point to pass threshold and the first point to pass threshold on the return, which is equivalent to an assigned duration of the number of sample points placed in the dwell times the sample interval. The probability density function (p.d.f.) for the dwell times is exponential with $y(t) = a \exp(-at)$. The record is digitized at interval T and the reduced data are obtained as histograms of the fraction of dwells containing N sample points, $Y(N)$. The goal is to derive an expression for $Y(N)$ in terms of $y(t)$ and T.

The starting point is the idea that N samples can be placed in a dwell time that lasts at least $(N-1)T$ and less than $(N+1)T$. $Y(N)$ for $N > 0$ is calculated from the sum

$$Y(N) = \int_{(N-1)T}^{NT} \text{prob}\,[N \text{ points placed in dwell of duration } t | \text{the dwell is of duration } t]$$

$$\times \text{prob}\,[\text{dwell is of duration } t]\,dt + \int_{NT}^{(N+1)T} \text{prob}\,[N|t]\,\text{prob}\,[t]\,dt. \qquad \text{(A 1.1)}$$

The conditional probability is zero outside the range $(N-1)T \leqslant d < (N+1)T$. Between $(N-1)T$ and NT it increases linearly as $(t\text{-}(N-1)T)/T$, then decreases linearly as $((N+1)T\text{-}t)/T$, since the sample grid is randomly located with respect to the start of events. The absolute probabilities are described by $y(t)$, so

$$Y(N) = \int_{(N-1)T}^{NT} (t\text{-}(N-1)T)/Ta \exp(-at)\, dt + \int_{NT}^{(N+1)T} ((N+1)T\text{-}t)/T\, a \exp(-at)\, dt.$$

Evaluating the integrals gives

$$Y(N) = \exp(-aT(N-1))\,(1-\exp(-aT))^2/aT, \quad N > 0,$$
$$Y(0) = (\exp(-aT)+aT\text{-}1)/aT,$$

where $Y(N)$ is the fraction of dwells given a duration of N sample points. The probability that the original duration was between NT and $(N+1)T$ long is

$$P(N) = \int_{NT}^{(N+1)T} a \exp(-at)\, dt = \exp(-aTN)\,(1-\exp(-aT)).$$

Note that the amplitude of the digitized probability mass function is low for the ' zero duration ' bin and high for all subsequent bins. This shift results from the basic definition of dwell time. More brief duration dwells are ' promoted ' to longer digitized durations than are ' demoted ' when the p.d.f. declines rapidly with respect to the sample interval. The ' promotion ratio ' is

$$Y(N)/P(N) = \exp(aT)\,(1-\exp(-aT))/aT = (\exp(aT)\text{-}1)/aT, \quad N \geqslant 1.$$

Dr Carol Vandenberg (personal communication) has obtained this same result by a more elegant method using convolutions of a uniform p.d.f. over T (sampling) with an exponential p.d.f. (event duration).

1.B. Closer to real data. Actual data have two additional sources of distortion. These are noise and time response. For a relatively simple method of detecting transitions and measuring dwells, and if the noise is assumed to be independent of the state of the system, it is likely that random noise will be self-cancelling and we will not consider it further. Colquhoun & Sigworth (1983; section 4.2.1) have considered this problem in more general terms, including the effects of noise.

A time constant in the recording apparatus will, however, distort the experimental histograms by decreasing the duration of transitions past threshold. The ' lost time ' redistributes from a dwell time with short mean duration into the distribution of dwell times in another recognizable state (e.g. closed to open). It is assumed that only one recognizable state (e.g. closed) has such a brief dwell-time component in this derivation. All of the assumptions and definitions from the preceding section apply, and in addition a simple exponential system response with time constant q is assumed. The following steps were taken. First, a modified p.d.f. was derived for dwell times above this threshold, which is defined as $n(d)$. This modified p.d.f. was then used to numerically evaluate a digitized ' dwell-time histogram.'

$n(d)$ was obtained by recognizing that a duration must exceed a minimum time, Z, to even reach threshold, where $Z = q \ln(2)$. The length of time above threshold, d, for duration t, given $t \geqslant Z$ is

$$d = t + q \ln(1-\exp(t/q)), \quad t \geqslant Z.$$

The inverse relationship is

$$t = q \ln (1+\exp (d/q)), \quad d \geqslant 0, t \geqslant Z.$$

To calculate $n(d)$, a function was first derived for the probability that a duration above threshold lasts less than or equal to d, from the original p.d.f., $y(t)$, and the expression relating true duration to time above threshold:

$$N(d) = \text{prob}[\text{duration above threshold} \leqslant d].$$

If the true duration is less than the minimum, the time above threshold is 0, so $N(0)$ is the area of $y(t)$ from 0 to Z. For true durations longer than Z, $N(d)$ was obtained by integrating $y(t)$ from Z to $q \ln (1+\exp (d/q))$.
This results in the expression

$$n(d) = 1-(1+\exp (d/q))^{-aq}.$$

A density function, $n(d)$ is obtained for $d > 0$ by differentiating (1-$N(d)$), to give

$$n(d) = a \exp (d/q)/[(1+\exp (d/q))^{(1+aq)}] \quad d > 0.$$

The digitized histogram, $W(N)$, could not be obtained in analytical form. Instead, it was calculated numerically from eqn. (A 1.1).

1.C. Practical considerations. Calculated values for $P(N)$, $Y(N)$ and $W(N)$ are shown in Fig. 11 for values appropriate to our data: sample interval (T) = 25 μs, mean duration (a) = 50 μs and filter time constant (q) = 40 μs. Clearly, the presence of an R-C filter boosts the number of undetected dwells and depresses the number of detected ones. Our strategy sets a conservative definition for the minimal accepted dwell (100 μs) and corrects the fitted amplitudes for the distortion introduced by digitization. Fitting of transitions using the system response characteristics (Colquhoun & Sakmann, 1981; Colquhoun & Sigworth, 1983) provides greater temporal resolution of brief dwell times. However, it was not clear what the effects of noise and a finite-system response time would be on the apparent duration of partially resolved dwells. Therefore, we have adopted a less sensitive but more conservative method of data reduction.

APPENDIX 2

Extraction of estimates for rate constants from data obtained from patches with many channels

Colquhoun & Hawkes (1981) have presented an approach for analysing single-channel current records obtained from patches with only one channel present, but it has been suggested that their approach is not appropriate when many channels are present (Dionne & Leibowitz, 1982). This Appendix presents a derivation, based on that of Colquhoun & Hawkes (1981), extending their approach to the analysis of closed-time histograms from many-channel patches in the low concentration limit. The approach is clear from the equations presented by Colquhoun & Hawkes (1981) and will only be outlined here. Jackson (1985) has recently presented a general derivation for the behaviour of a many-channel patch. The derivation is presented first for a three-state linear scheme, since the derivation is more intuitive; then it is extended to longer linear schemes. The goal is to calculate the distribution of

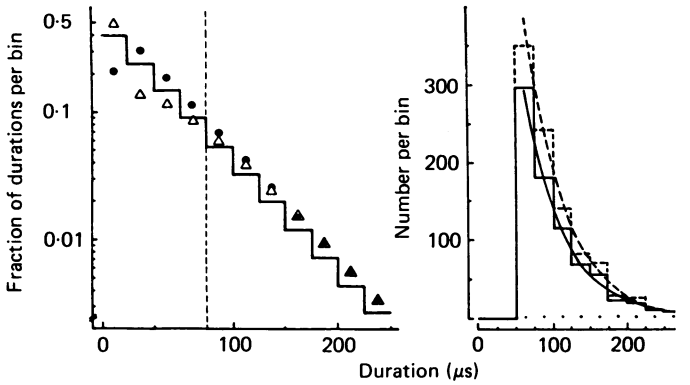

Fig. 11. The left panel shows a semilogarithmic plot of numerical evaluations of three probability mass functions, that of the original durations, $P(N)$ (histogram), the digitized durations, $Y(N)$ (●), and durations digitized from data recorded in the presence of an R–C filter, $W(N)$ (△), generated as described in Appendix 1. The bin size (T) used was 25 μs, the characteristic time of the underlying p.d.f. (a) 50 μs and the time constant for the apparatus (q) 40 μs. The vertical dashed line indicates the minimal acceptable dwell used in our data reduction (75 or 100 μs). The right panel shows the short-duration 'closed-duration' histogram for synthesized data generated using a single channel following a three-state scheme. The synthesis was done using rates (see A 2.2 for definitions, rates in s^{-1}): $f = 100$, $r = 10000$, $b = 10000$, $a = 400$. The purpose of the simulation is to illustrate the effects of digitization described in Appendix 1. The original data are shown by the continuous histogram and line, whereas the dashed histogram and line show results when the data were 'digitized' at 25 μs intervals with 50 μs minimal open and closed times (the original data have had the first two bins blanked). Note the increase in numbers of brief 'detected' events. The continuous line was generated using the predicted numbers and rate constants for the two exponential components in the closed-time histogram (see Appendix 2): the slower component is not seen at this time scale. The dashed line has had the amplitude of the brief component scaled by the predicted factor (1·29).

periods between the time of closing of a single channel which brings all channels to a closed state and the first subsequent opening.

This distribution is

$$K(t) = \text{prob}\,[\text{a closed period lasts} \leqslant t | \text{one channel closed at time 0 and all channels were closed at 0}],$$

(for simplicity, the conditional notation will be dropped).

However, it is easier to calculate the quantity

$$\begin{aligned} J(t) &= 1\text{-}K(t), \\ &= \text{prob}\,[\text{a closed period lasts} > t], \\ &= \text{prob}\,[\text{no openings 0 to } t]. \end{aligned}$$

With N independent channels present, this can be written as

$$\begin{aligned} J(t) = \text{prob}\,[&\text{channel 1 does not open 0 to } t \text{ and channel 2 does not open 0 to } t \ldots \\ &\text{and channel } N \text{ does not open 0 to } t], \\ = \text{prob}\,[&\text{channel 1 does not open 0 to } t] \times \ldots \times \text{prob}\,[\text{channel } N \text{ does not open 0 to } t]. \end{aligned} \quad \text{(A 2.1)}$$

To derive an expression for $J(t)$, the N channels are assumed to be identical and independent. In the derivation, they are assumed to follow scheme (A 2.2)

$$\overset{\text{(closed)}}{0} \underset{r}{\overset{f}{\rightleftharpoons}} \overset{\text{(closed)}}{1} \underset{a}{\overset{b}{\rightleftharpoons}} \overset{\text{(open)}}{2} \qquad \text{(A 2.2)}$$

The forward binding rate (f) includes the concentration term, and in the low concentration limit $f \ll r$.

The N channels are divided in two groups, the one which just closed and $(N-1)$ channels at equilibrium among the closed states. The derivation proceeds by calculating $J(t)$ from conditional probability density functions for the two groups of channels, then obtaining the conditional p.d.f. for the N-channel system by differentiating $(1\text{-}J(t))$.

For the channel which just closed, the conditional p.d.f. for dwell times in closed states (0 and 1) given the channel is in state 1 at $t = 0$ and the open state (2) is absorbing (see Colquhoun & Hawkes, 1981), is

$$p_1(t) = A_1 \exp(-a_1 t) + A_2 (\exp(-a_2 t), \qquad \text{(A 2.3)}$$

where

$$\begin{aligned} a_1 &= (z_1 - z_2)/2, \\ a_2 &= (z_1 + z_2)/2, \\ z_1 &= f + r + b, \\ z_2 &= (z_1\, z_1 - 4fb)^{\frac{1}{2}}, \qquad \text{(see scheme A 2.2)} \\ A_1 &= b\,(f\text{-}a_1)/(a_2\text{-}a_1), \\ A_2 &= b(a_2\text{-}f)/(a_2\text{-}a_1). \end{aligned}$$

The probability distribution function for closed periods is the integral of $p_1(t)$ from 0 to t,

$$\begin{aligned} p'_{1\,(t)} &= 1 - Q_1 \exp(-a_1 t) - Q_2 \exp(-a_2 t), \\ Q_1 &= A_1/a_1, \\ Q_2 &= A_2/a_2. \end{aligned}$$

The desired function is the probability that a closed period lasts longer than t:

$$p_1(t) = 1 - p'_1(t) = Q_1 \exp(-a_1 t) + Q_2 \exp(-a_2 t). \qquad \text{(A 2.4)}$$

The other $(N-1)$ channels are distributed at equilibrium between closed states 0 and 1. The channels in state 1 (bound and closed) are neglected because the low concentration limit is assumed. Analogous calculations give a distribution for the first opening of a single channel in this equilibrium population, starting in state 0,

$$p_E(t) = M[\exp(-a_1 t)/a_1 - \exp(-a_2 t)/a_2],$$

where,

$$M = bf/(a_2 - a_1) \text{ (see A 2.2 and A 2.3 for definition).}$$

In the low concentration limit $a_1 \ll a_2$, so the second exponential is negligible with respect to the first at all times, and

$$p_E(t) = M \exp(-a_1 t)/a_1. \qquad \text{(A 2.5)}$$

It is now easy to obtain $J(t)$, by multiplying the distributions for all N channels

$$J(t) = p_1(t) \times p_E(t) \times \ldots \times p_E(t),$$
$$= p_1(t)\, p_E(t)^{(N-1)}.$$

The probability distribution function for closed times for the N channels is $K(t) = 1 - J(t)$, and the desired probability density function is

$$k(t) = dK(t)/dt = Q_1 S \exp(-St) + Q_2 F \exp(-Ft), \qquad \text{(A 2.6)}$$

where $S = Na_1$ and $F = (N-1)a_1 + a_2$. Integration of $k(t)$ over intervals of a sample interval gives the predicted closed-time histograms. Note that this result is the same obtained by Colquhoun & Hawkes (1981) when $N = 1$, and is essentially identical to equations 14 and 17 of Jackson (1985).

Referring back to the definitions, the measurable parameters can be related to the underlying system parameters as follows. Two components will be seen in the closed-time histogram.

$F = (N-1)a_1 + a_2$ is the decay rate of the briefer component,
$S = Na_1$ is the decay rate of the longer component.

If $N \gg 1$, then $a_2 = F$–S. Also, practically, $S \ll F$ for our records. S can approach F for two reasons: $N \gg 1$ or $(N-1)a_1$ approaches a_2. If N is very large, then a_2 can be derived. If N is small but $(N-1)a_1$ approaches a_2, the low concentration limit is violated. The assumption of the low concentration limit and/or of large N must be independently justified. In the low concentration limit $f \ll r$, $a_1 \ll a_2$ and $f \ll a_2$, so

$$a_1 = fb/(b+r),$$
$$a_2 = b + r.$$

The areas of the two components are

$Q_2 = b(a_2\text{-}f)/((a_2\text{–}a_1)a_2)$ fraction of dwells in brief component,
$Q_1 = b(f\text{-}a_1)/((a_2\text{–}a_1)a_1)$ fraction of dwells in long component.

In the low concentration limit, $Q_2 = b/a_2 = b/(r+b)$ and $Q_1 = r/(r+b)$.

Using these relationships two rates can be derived from the data:

$$b = Q_2(F\text{–}S) = \text{opening rate},$$
$$r = Q_1(F\text{–}S) = \text{unbinding rate}. \qquad \text{(A 2.7)}$$

The rate S is an 'effective opening rate' for the equilibrium population of closed channels. In the low concentration limit, $S = Na_1 = Nfb/(b+r)$. The two components in the closed-time histogram reflect two underlying processes: the relaxation of the just-closed channel from state 1 (reopenings after a brief closure) and the behaviour of the equilibrium population largely in state 0 (including the just-closed channel when it loses ligand rather than reopening).

The extension of this analysis to a four-state linear scheme is immediate, although it is less intuitive because justifying the dropping of some terms is not necessarily obvious. Again, in the low concentration limit, it is assumed that essentially all closed

channels are in the unbound state (R in text scheme (1). The resulting closed-time histogram again shows two exponential components. Using the same notation for experimental values and the notation for rates given in text scheme (1), in the low concentration limit

$$\begin{aligned} F &= \beta + k_{-2} + S, \\ S &= N(k_2\, k_1/k_{-1})\,(\beta/(\beta + k_{-2})), \\ Q_2 &= \beta/(\beta + k_{-2}), \\ Q_1 &= k_{-2}/(\beta + k_{-2}). \end{aligned} \qquad \text{(A 2.8)}$$

This analysis gives an identical result to the approach presented by Colquhoun & Sakmann (1981). The decay rate of the brief component is identically defined. The number of ' gaps per burst ' is given by $Q_2/Q_1 = \beta/k_{-2}$, since for every ' burst ' there must be a defining long-duration closed time.

The equations presented by Dionne & Leibowitz (1982) appear to be quite different. In fact, as originally presented they make incorrect predictions for the amplitude and decay rate of the long-duration component of the closed-time histogram. However, if the value for S (eqn. A 2.8) is used as the effective opening rate for the equilibrium population of closed channels in the derivation given by Dionne & Leibowitz, (1982), then the predictions agree with those given here and with the results of stochastic simulations of channel behaviour. Dionne & Leibowitz (1982) use an effective opening rate of $N\beta k_1 k_2/(k_{-1}k_{-2})$, rather than S. Clearly, the divergence between the equations presented here and those of Dionne & Leibowitz (1982) increases as β increases with respect to k_{-2}. The value for S can be derived in another way. In the low concentration limit most receptors are unliganded, so the mean dwell time in closed states for the equilibrium population of closed receptors should be very close to the mean time for a receptor starting in R to reach A_2R^*. This time is $k_{-1}(\beta + k_{-2})/(k_1 k_2 \beta)$ (e.g. Colquhoun & Hawkes (1981), eqns. (3.60)–(3.72), with k_1, $k_2 \ll k_{-1}$, k_{-2}). For a single channel, therefore, the opening rate will be the inverse of this mean time, and for N channels the frequency of bursts will be S.

The ability of these equations to describe records was assessed by stochastic simulation of a four-state linear scheme. The predictions are quite close to the simulations (Fig. 12). Dr M. Leibowitz also kindly provided histograms resulting from independent simulation (see Leibowitz & Dionne, 1984) which were equally well described (data not shown). Repeated simulations at increasing ' agonist concentrations ' were made to qualitatively estimate the extent of the low concentration range. Good predictions were made when 99% of receptors with closed channels were in the R state. When the percentage dropped to 95%, the predictions deviated noticeably from the data. With the synthesized data, the deviation could be ascribed to the presence of an additional exponential component. Analysis of the histograms, however, did not clearly reveal this additional component, but instead the data could be ' satisfactorily fitted ' by a sum of two exponentials, as two components had time constants less than 3-fold different. Clearly, therefore, the observation that data appear to contain only two-exponential closed-time components does not imply that the low concentration limit applies, nor that the data may be validly interpreted as outlined here.

The closed-time histograms do not contain any information about multiple

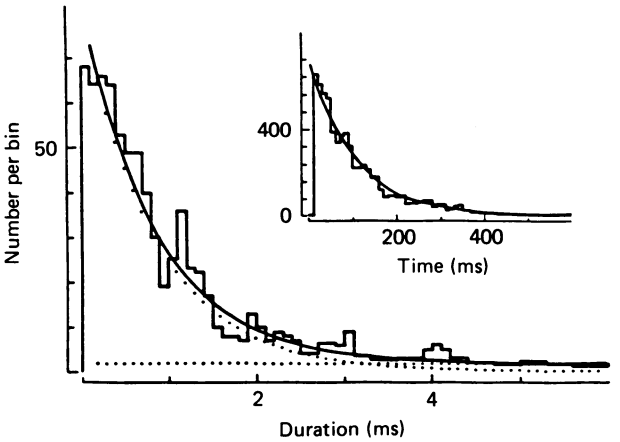

Fig. 12. This figure shows a closed-time histogram resulting from a stochastic simulation of a four-state linear scheme (scheme (1)). The histogram was generated from the original simulated data, and so is not affected by digitization. The main panel shows short-duration closings (bin size 100 μs), the inset longer-duration closings (bin size 10 ms, first bin blanked). The continuous curve shows the sum of two calculated exponentials, the dotted curves in the main panel show the two calculated curves. The simulation had 1550 channels present, and the histogram contains 2620 entries. The concentration of hypothetical agonist used was 10^{-7} M, and the rates (in s^{-1}) were: $k_1 = 1{\cdot}43$; $k_2 = 14{\cdot}3$; $k_{-1} = 860$; $k_{-2} = 860$; $\beta = 321$; ($\alpha = 30$).

The theoretical curves were calculated with parameters: $S = Na_1 = 1550 \times 0{\cdot}00642 = 9{\cdot}95$; $F = \beta + k_{-2} + S = 1191$; $Q1 = \beta/(\beta + k_{-2}) = 0{\cdot}272$.

The ' effective opening rate ' (compare to S) is: $N\beta k_1 k_2/(k_{-1}(\beta + k_{-2})) = 10{\cdot}01$.

The histograms were fitted with our analysis programs, giving estimates: $S = 10{\cdot}26$; $F = 1140$; $Q_1 = 0{\cdot}274$; $\beta = 310$ (value used 321); $k_{-2} = 820$ (value used 860).

For ten simulations the mean β fit was 314 ± 19 (290–350) and the mean k_{-2} was 834 ± 35 (765–880).

openings (times when more than one channel is open) and the derivation takes no account of their presence. Multiple openings are not a problem as long as they are rare. If multiple openings are very common, the derivation may be inapplicable because it was assumed that the $N-1$ channels which were already closed were at equilibrium and, in the low concentration limit, unliganded. If multiple openings are very common, then it is more likely that one or more of the $N-1$ channels had just closed and had not yet joined the equilibrium population of closed channels. If $1/S$ is long compared to $1/F$ then the presence of multiples should not affect the interpretation (i.e. if the mean time for an unliganded channel to open divided by the number of channels is long compared to the time taken for a just-closed channel to reopen or join the equilibrium population). All of our records have few multiples and also show a low probability that any channel is open, so that $1/S$ is long compared to $1/F$ and also long compared to the mean time it takes an open channel to join the equilibrium closed population. Under these conditions ' bursting ' is clearly apparent and separable from independent activations (e.g. Colquhoun & Sakmann, 1981). It is important to determine, however, that behaviour within bursts is constant across a record.

The shape of closed-time histograms depends on being able to resolve open states, but is less sensitive to missing short closed dwells (missed openings will alter amplitudes and decay constants, whereas missed closings will reduce the number of brief closed durations seen but not the shape of the curve for resolved closed periods). Indeed, a great problem in any data such as ours occurs if both resolvable states (open and closed) show brief dwell time components approaching the sample interval. At present, we have no satisfactory way to deal with this question. Our only comment, in terms of the data presented in this paper, is that both scrutiny of the raw data and analysis of the digitized data have led us to believe that brief openings are largely surrounded by long closed periods and brief closed periods by long openings. This conclusion, although we have not proven that it is accurate, minimizes the interactions of missed dwells in the two resolvable states.

S.M.S. was supported by a NIH Post-doctoral Fellowship. The research was supported by NIH grants NS-13719 and NS-22356. We thank Drs D. Colquhoun and B. Sakmann for discussions and for copies of manuscripts prior to publication, Dr Carol Vandenberg for helpful comments on the manuscript, and Drs V. E. Dionne and M.Leibowitz for discussions and the results of stochastic simulations of channel activation.

REFERENCES

ADAMS, P. R. (1981). Acetylcholine receptor kinetics. *Journal of Membrane Biology* **58**, 161–174.

AUERBACH, A. & SACHS, F. (1984). Single channel currents from acetylcholine receptors in embryonic chick muscle: kinetic and conductance properties of gaps within bursts. *Biophysical Journal* **45**, 187–198.

BRENNER, H. R. & SAKMANN, B. (1983). Neurotrophic control of channel properties at neuromuscular synapses of rat muscle. *Journal of Physiology* **337**, 159–171.

CASH, D. J., AOSHIMA, J. & HESS, G. P. (1981). Acetylcholine induced cation translocation across cell membranes and inactivation of the acetylcholine receptor: chemical kinetic measurements on the millisecond time region. *Proceedings of the National Academy of Sciences of the U.S.A.* **78**, 3318–3322.

COLQUHOUN, D., DREYER, F. & SHERIDAN, R. E. (1979). The actions of tubocurarine at the frog neuromuscular junction. *Journal of Physiology* **293**, 247–284.

COLQUHOUN, D. & HAWKES, A. G. (1981). On the stochastic properties of single ion channels. *Proceedings of the Royal Society* B: **211**, 205–235.

COLQUHOUN, D. & SAKMANN, B. (1981). Fluctuations in the microsecond time range of the current through the single acetylcholine receptor ion channels. *Nature* **294**, 464–466.

COLQUHOUN, D. & SAKMANN, B. (1985). Fast events in single-channel currents activated by acetylcholine and its analogues at the frog muscle end-plate. *Journal of Physiology* **369**, 501–557.

COLQUHOUN, D. & SIGWORTH, F. J. (1983). Fitting and statistical analysis of single-channel records. In *Single-Channel Recording*, ed. SAKMANN, B. & NEHER, E., pp. 191–264. New York: Plenum Press.

DIONNE, V. & LEIBOWITZ, M. (1982). Acetylcholine receptor kinetics. A description from single channel currents at snake neuromuscular junctions. *Biophysical Journal* **39**, 253–261.

DIONNE, V. E., STEINBACH, J. H. & STEVENS, C. F. (1978). An analysis of the dose–response relationship at voltage-clamped frog neuromuscular junctions. *Journal of Physiology* **281**, 421–444.

DIONNE, V. E. & STEVENS, C. F. (1975). Voltage dependence of agonist effectiveness at the frog neuromuscular junction: resolution of a paradox. *Journal of Physiology* **251**, 245–270.

HAMILL, O. P., MARTY, A., NEHER, E., SAKMANN, B. & SIGWORTH, F. J. (1981). Improved patch-clamp techniques for high resolution current recording from cells and cell-free patches. *Pflügers Archiv* **391**, 85–100.

JACKSON, M. B. (1985). Stochastic behaviour of a many-channel membrane system. *Biophysical Journal* **47**, 129–137.

JACKSON, M., WONG, B., MORRIS, C., CHRISTIAN, C. & LECAR, H. (1983). Successive openings of the same acetylcholine receptor channel are correlated in open time. *Biophysical Journal* **42**, 109–114.

KATZ, B. & MILEDI, R. (1973). The characteristics of 'end-plate noise' produced by different depolarizing drugs. *Journal of Physiology* **230**, 707–717.

LEIBOWITZ, M. & DIONNE, V. (1984). Single channel acetylcholine receptor kinetics. *Biophysical Journal* **45**, 153–163.

LINDER, T. M., PENNEFATHER, P. & QUASTEL, D. M. J. (1984). The time course of miniature endplate currents and its modification by receptor blockade and ethanol. *Journal of General Physiology* **83**, 435–468.

MAGLEBY, K. L. & STEVENS, C. F. (1972). A quantitative description of end-plate currents. *Journal of Physiology* **223**, 151–171.

MORRIS, C. E., WONG, B. S., JACKSON, M. B. & LECAR, H. (1983). Single-channel currents activated by curare in cultured embryonic rat muscle. *Journal of Neuroscience* **3**, 2525–2531.

NEHER, E. & SAKMANN, B. (1975). Voltage-dependence of drug-induced conductance in frog neuromuscular junction. *Proceedings of the National Academy of Sciences of the U.S.A.* **72**, 2140–2144.

PATRICK, J., MCMILLAN, J., WOLFSON, H. & O'BRIEN, J. C. (1977). Acetylcholine receptor metabolism in a nonfusing muscle cell line. *Journal of Biological Chemistry* **252**, 2143–2153.

QUAST, U., SCHIMERLIK, M., LEE, T., WITZEMANN, V., BLANCHARD, S. & RAFTERY, M. A. (1978). Ligand-induced conformation changes in *Torpedo californica* membrane-bound acetylcholine receptor. *Biochemistry* **17**, 2405–2414.

REDMANN, G., ADAMS, P. R. & CLARK, R. B. (1982). Conduction and kinetics of single acetylcholine channels in a cultured mammalian cell. *Neuroscience Abstracts* **8**, 718.

SAKMANN, B. & NEHER, E. (1983). Geometric parameters of pipettes and membrane patches. In *Single-Channel Recording*, ed. SAKMANN, B. & NEHER, E., pp. 37–52. New York: Plenum Press.

SIEGELBAUM, S. A., TRAUTMANN, A. & KOENIG, J. (1984). Single acetylcholine-activated channel currents in developing muscle cells. *Developmental Biology* **104**, 366–379.

SINE, S. M. & STEINBACH, J. H. (1984*a*). Activation of a nicotinic acetylcholine receptor. *Biophysical Journal* **45**, 175–185.

SINE, S. M. & STEINBACH, J. H. (1984*b*). Agonists block currents through acetylcholine receptor channels. *Biophysical Journal* **46**, 277–284.

SINE, S. M. & STEINBACH, J. H. (1986). Acetylcholine receptor activation by a site-selective ligand: nature of brief open and closed states in BC3H-1 cells. *Journal of Physiology* **370**, 357–379.

SINE, S. M. & TAYLOR, P. (1979). Functional consequences of agonist-mediated state transitions in the cholinergic receptor. Studies on cultured muscle cells. *Journal of Biological Chemistry* **254**, 3315–3325.

SINE, S. M. & TAYLOR, P. (1980). The relationship between agonist occupation and the permeability response of the cholinergic receptor revealed by bound cobra α-toxin. *Journal of Biological Chemistry* **255**, 10144–10156.

SINE, S. M. & TAYLOR, P. (1981). Relationship between reversible antagonist occupancy and the functional capacity of the acetylcholine receptor. *Journal of Biological Chemistry* **256**, 6692–6699.

STEINBACH, J. H. (1980). Activation of nicotinic acetylcholine receptors. *Cell Surface Review* **6**, 120–157.

TRAUTMANN, A. & SIEGELBAUM, S. A. (1983). The influence of membrane patch isolation on single acetylcholine-channel current in rat myotubes. In *Single Channel Recording*, ed. SAKMANN, B. & NEHER, E. pp. 473–480. New York: Plenum Press.

WEILAND, G. & TAYLOR, P. (1979). Ligand specificity of state transitions in the cholinergic receptor: behaviour of agonists and antagonists. *Molecular Pharmacology* **15**, 197–212.